# 70081: Immobilization of Radionuclides in the Hanford Vadose Zone by Incorporation in Solid Phases

Samuel J. Traina[1], Philip Grandinetti[1], Isao Yamakawa[1],

Subramanian Prasad[1], Yongtian He[1],

Gordon E. Brown, Jr.[2,3], Jefferey G. Catalano[2], Jefferey A. Warner[2],

Calvin C. Ainsworth[4], Nikolla P. Qafoku[4] and Jim E. Szecsody[4]

1 2 3 4

PNNL

# Hypothesis

Reaction of hyper-alkaline Na-aluminate fluids (from the REDOX tank wastes) with subsurface geomaterials results in novel chemistry leading to transformation/immobilization of radio-isotopes and hazardous metals.

# Objectives

1. Evaluate the polymerization/precipitation of Al-(hydr)oxides and possible incorporation of contaminant metals.

2. Evaluate the dissolution/reprecipitation of Al-silicates and possible incorporation of contaminant metals, with model solids and Hanford sediments.

3. Evaluate the geochemistry/transport of select contaminants in Hanford sediments impacted by tank waste simulants.

4. Ground-truth lab studies with direct speciation of contaminated sediments from the Hanford site.

# Al polymerization/precipitation and contaminant incorporation

- Al-polymers/precipitates examined with $^{27}$Al NMR, Al K-edge XANES and XRD

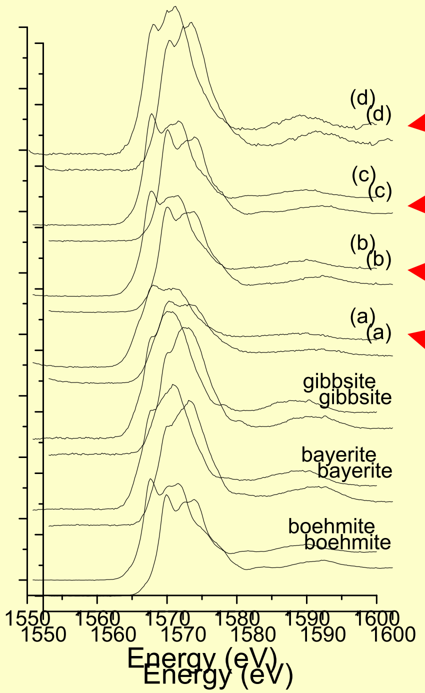


80°C, 7 days OH/Al = 4.0, 10 m*M* $NaNO_3$

80°C, 3 days OH/Al = 4.0, 10 m*M* $NaNO_3$

fresh precipitate, OH/Al = 4.0, 2 *M* $NaNO_3$

fresh precipitate, OH/Al = 4.0, 10 m*M* $NaNO_3$

# Al polymerization/precipitation and contaminant incorporation: Sr sorption on powders at pH 10

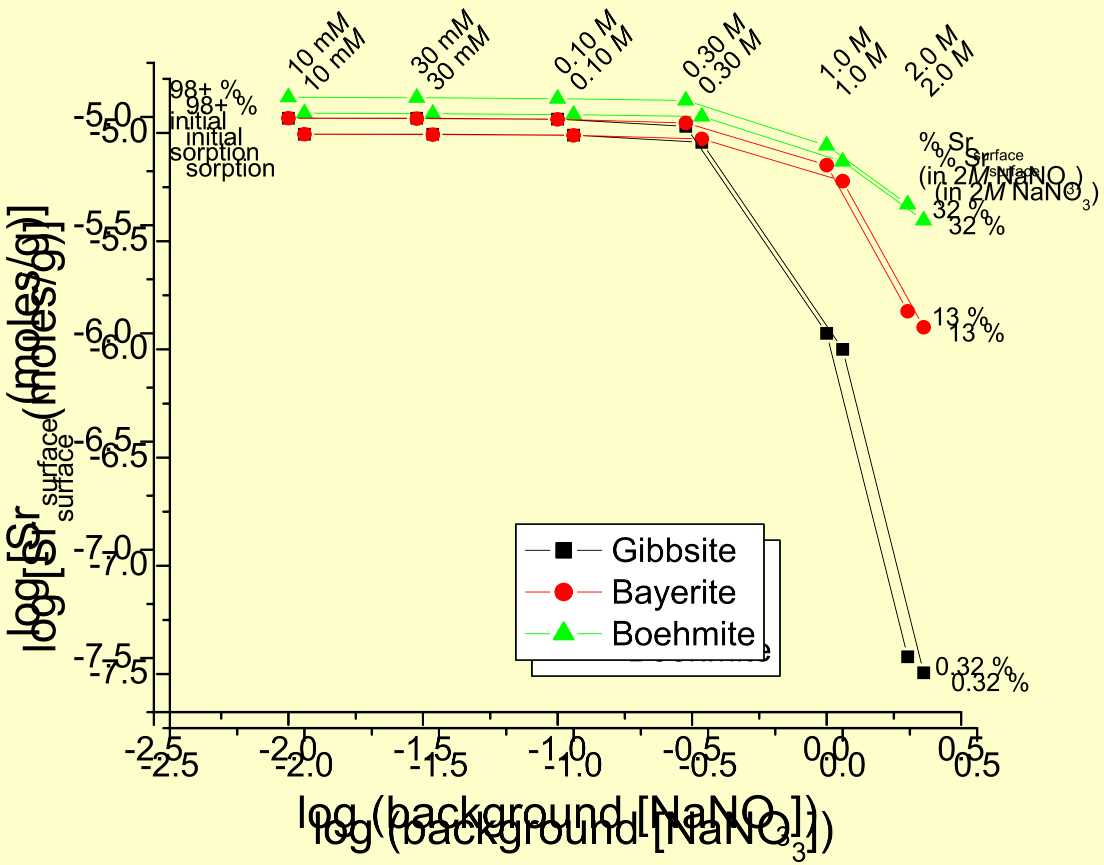


- Competition with $Na^+$ evident

- Greater sorption by boehmite than gibbsite

# Al polymerization/precipitation and contaminant incorporation: Sr sorption on gels

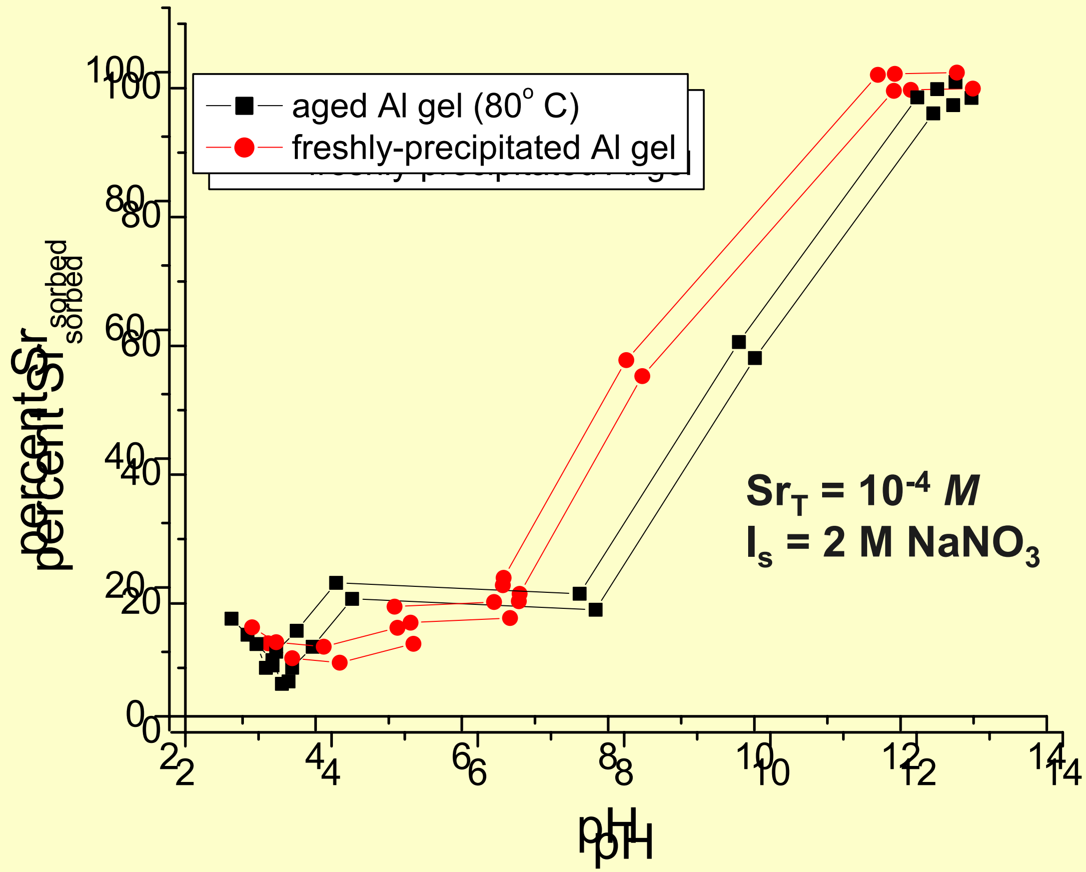

# Al polymerization/precipitation and contaminant incorporation:  Sr sorption on gels at pH 10

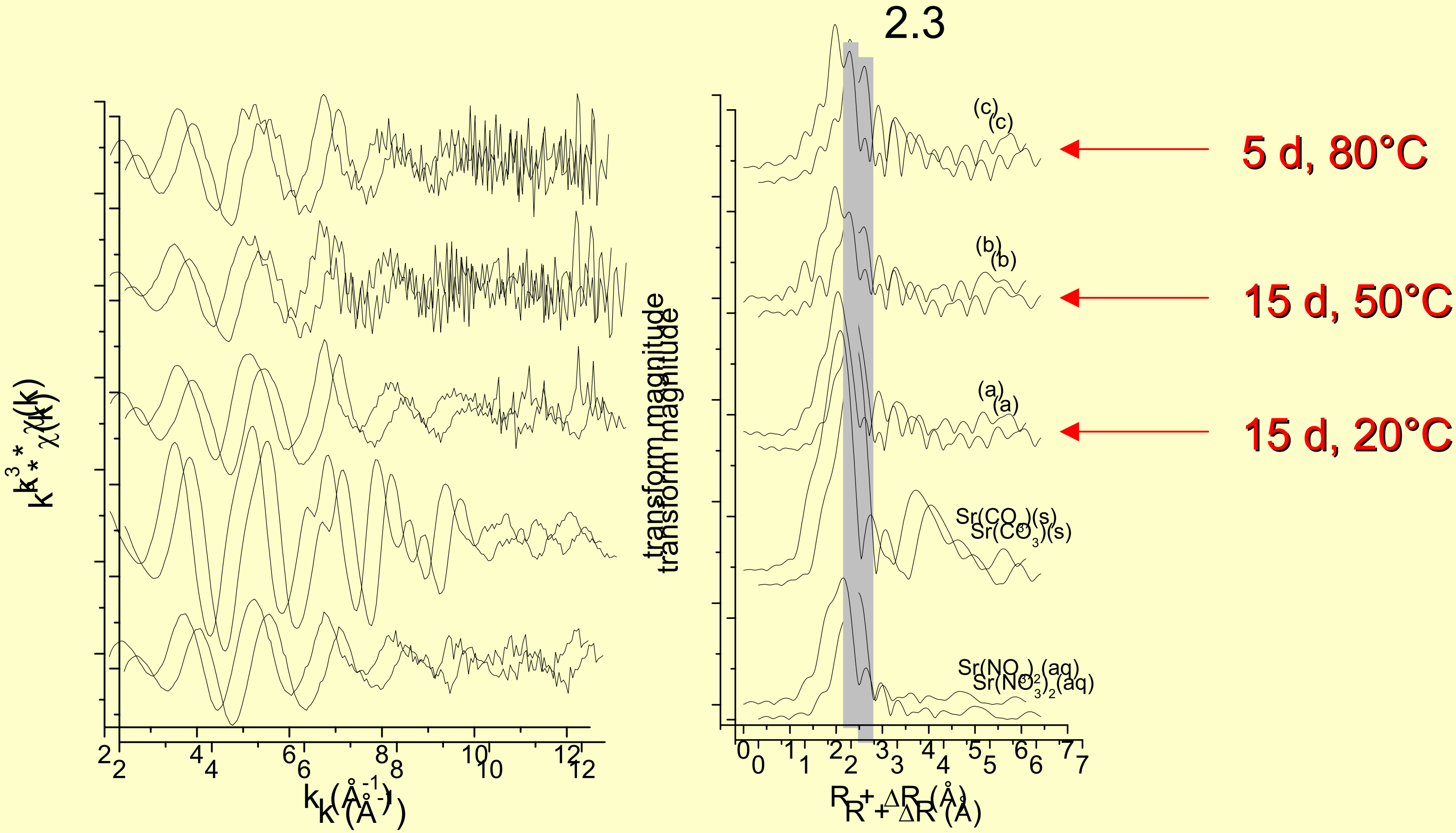

# Oxidation of Co(II) to Co(III) in the Presence of Hanford Sediments: Inhibition by Fe(II)-bearing Minerals

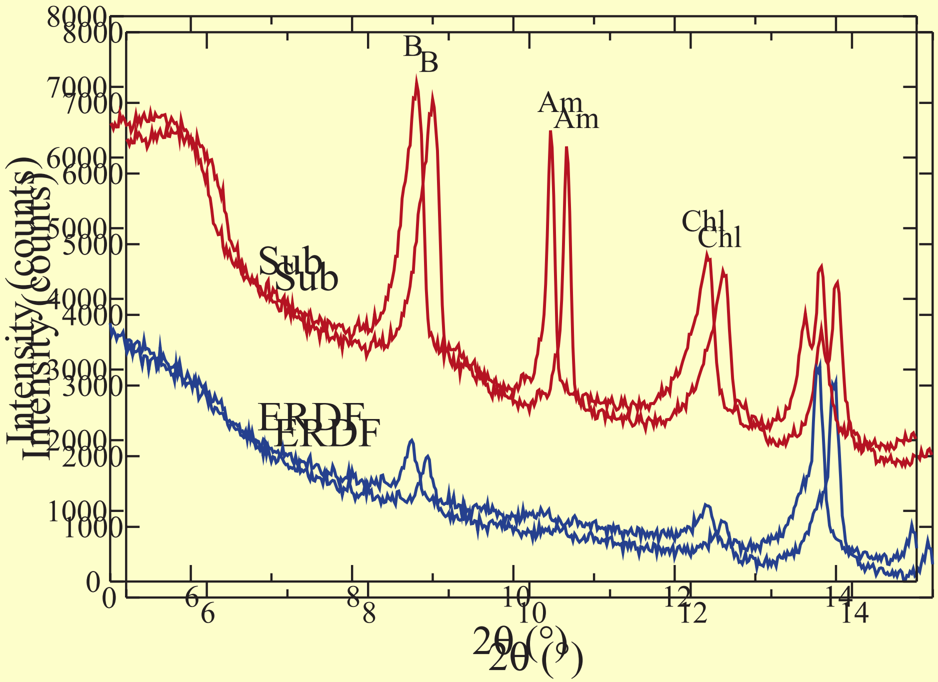


Two Hanford sediment samples used:

(1) From the ERDF pit, fine sand ⇒ **ERDF**

(2) From the Submarine pit, fine sandy silt ⇒ **Sub**

Both sediments predominantly quartz and feldspar

Sub sediment contains more Fe(II)-bearing minerals: biotite (**B**), amphibole (**Am**), and chlorite (**Chl**) based on powder XRD (right)

Powder XRD of sediments

# Aqueous Co(II) reacted with the two Hanford sediment samples at pH 12 in 1 M $NaNO_3$, analyzed by XAFS:

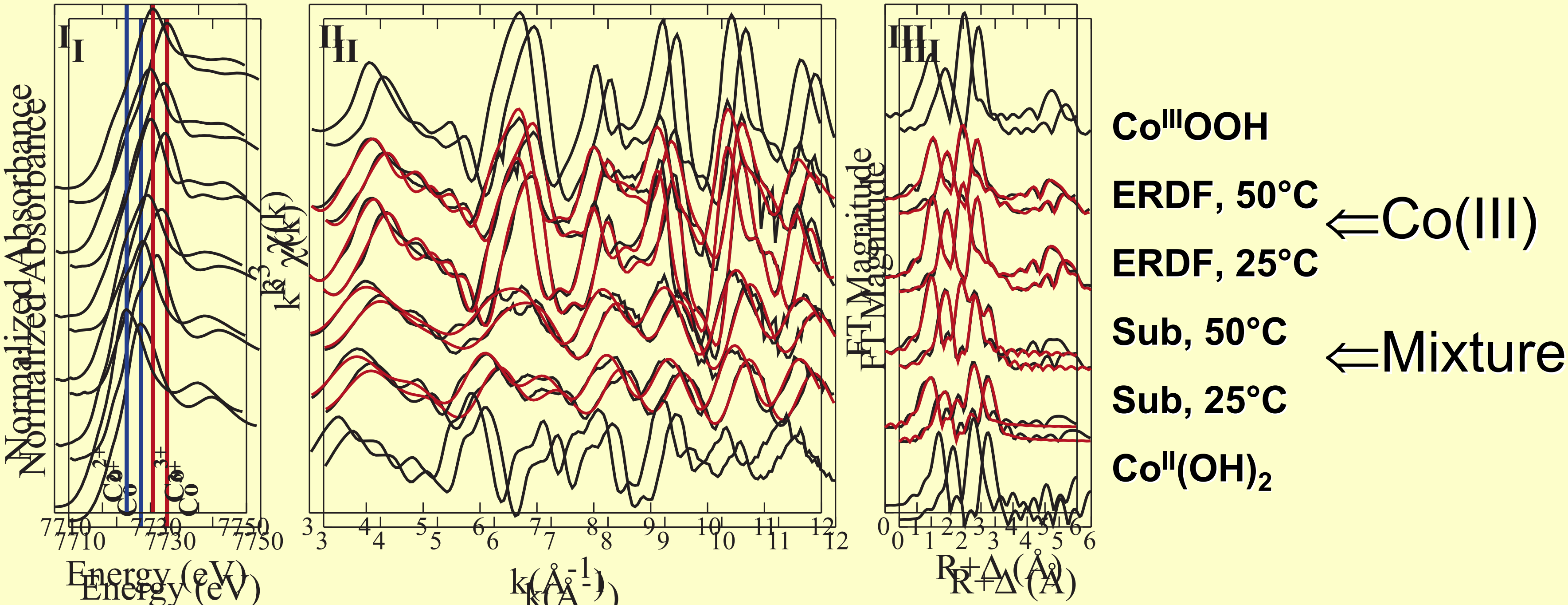


- Co(II) oxidizes to Co(III) in the ERDF sediments
- A mixture of Co(II) and Co(III) forms in the Sub sediments
- **Suggests Co oxidation is partially inhibited by Fe(II) minerals**

$UO_2^{2+} + H_2O = UO_2OH^+ + H^+$

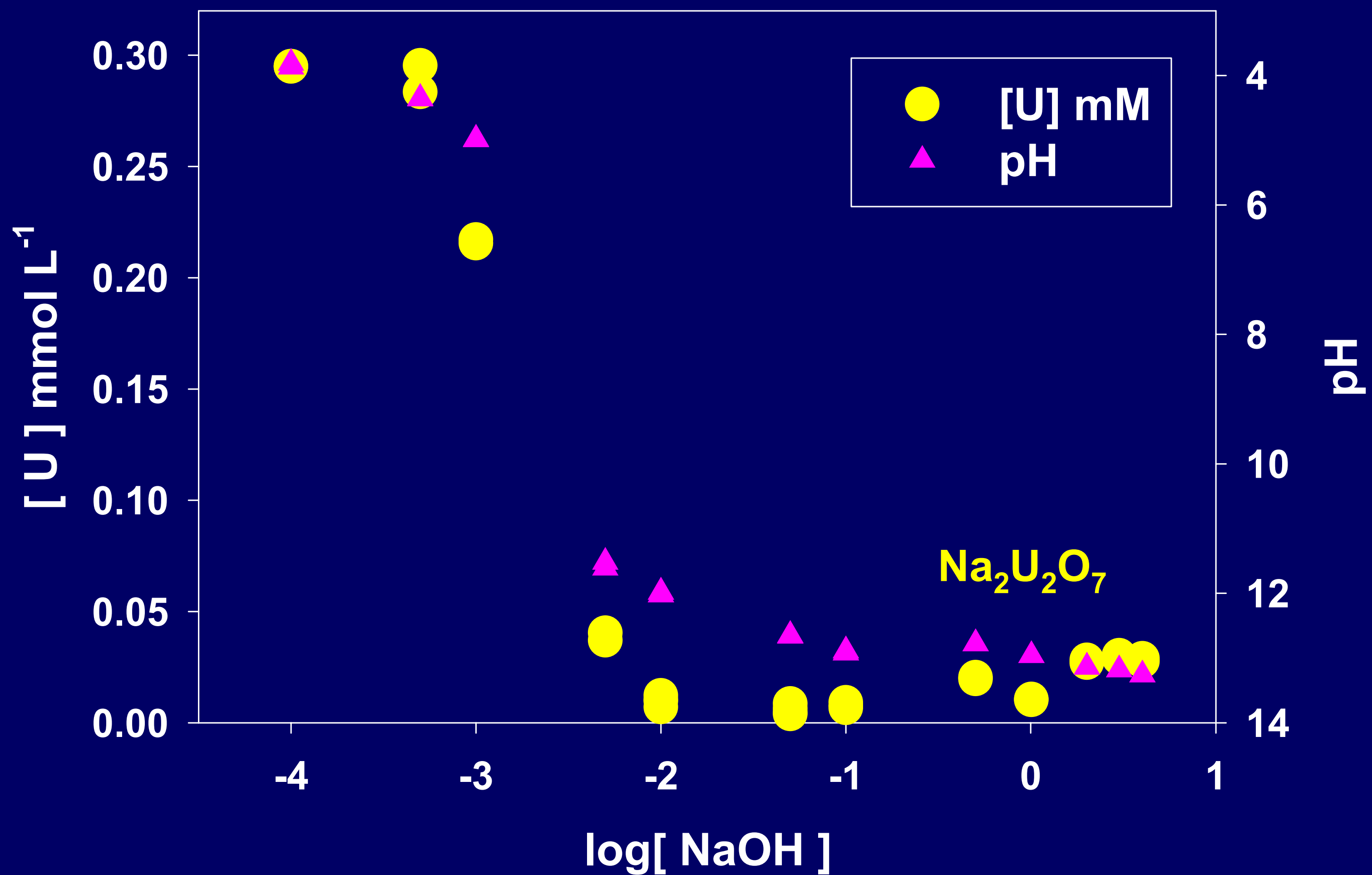

# $CO_3^{2-}$ effect on U solubility

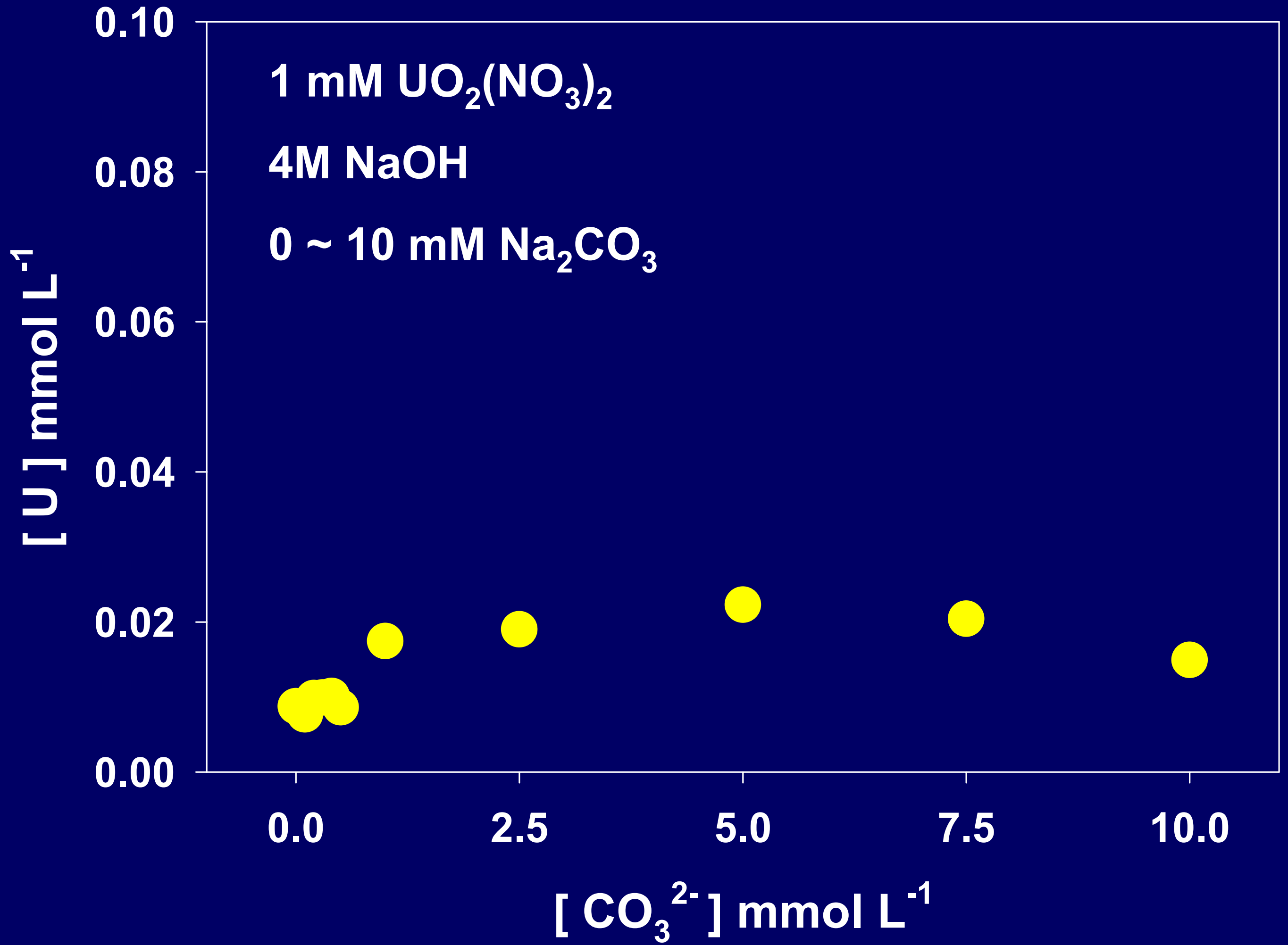

# $Na_2U_2O_7$ solubility, logK=22.59

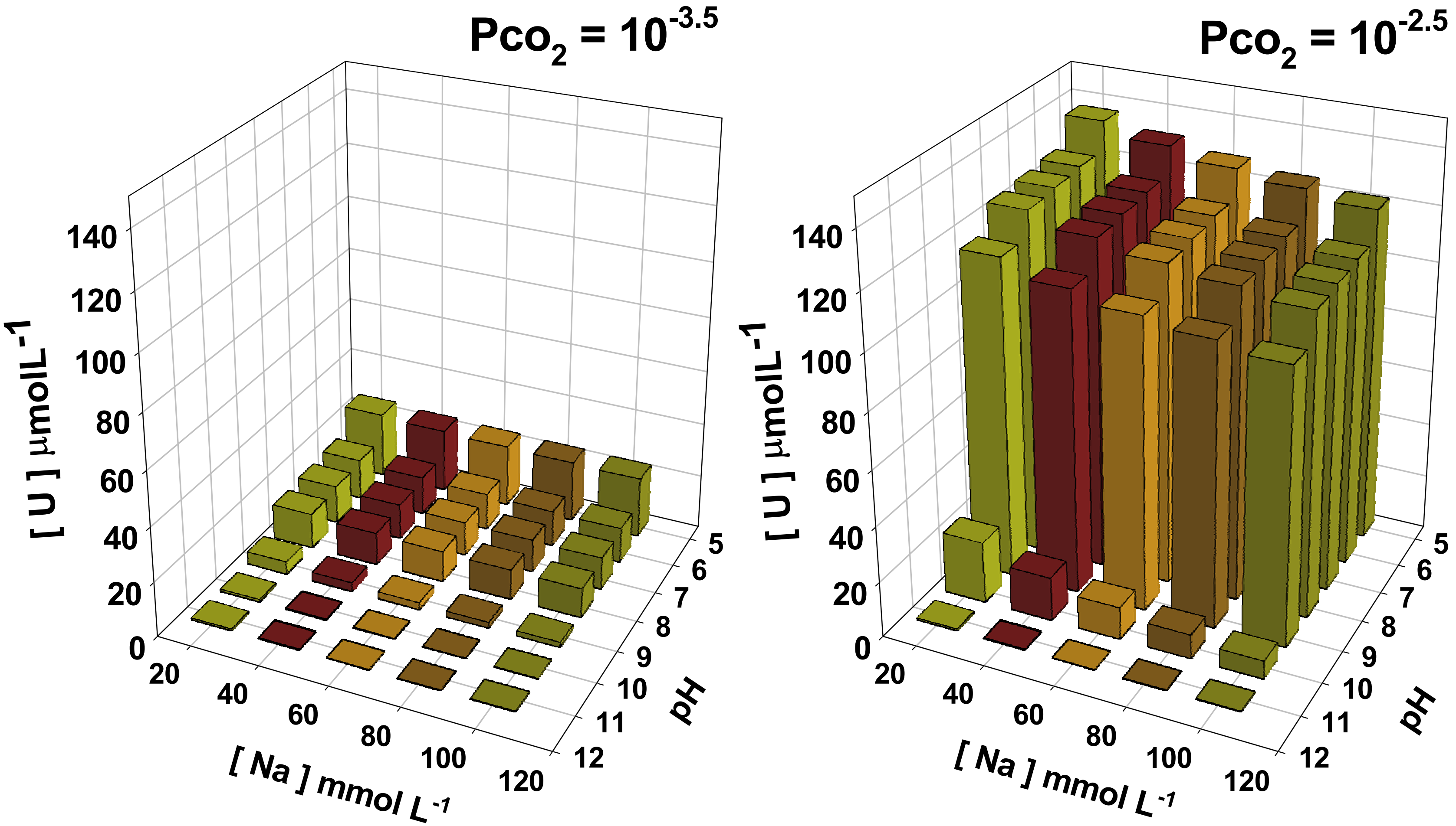

## $2UO_2^{2+} + 2Na^+ + 2OH^- + H_2O = Na_2U_2O_7 + 4H^+$

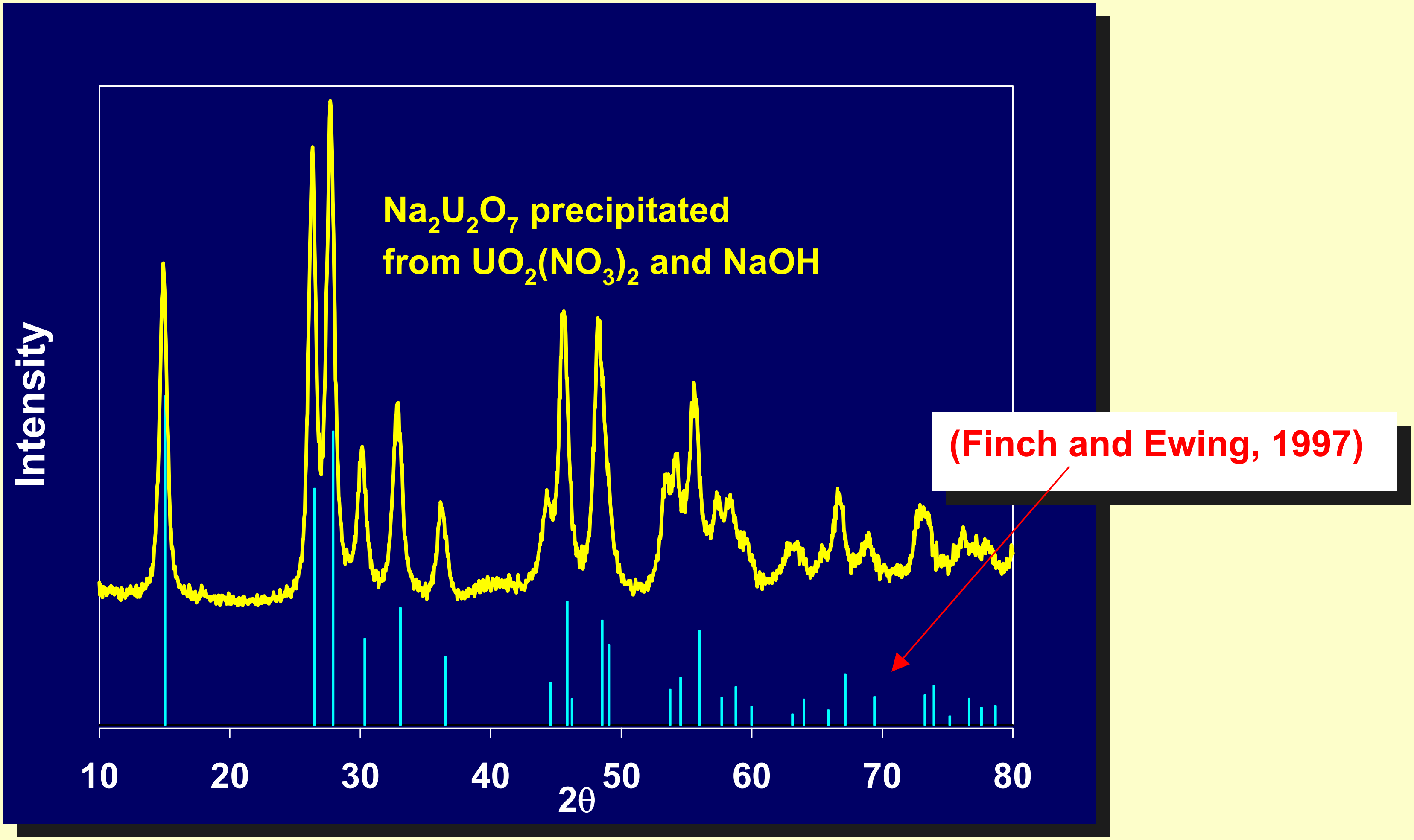

# XRD patterns

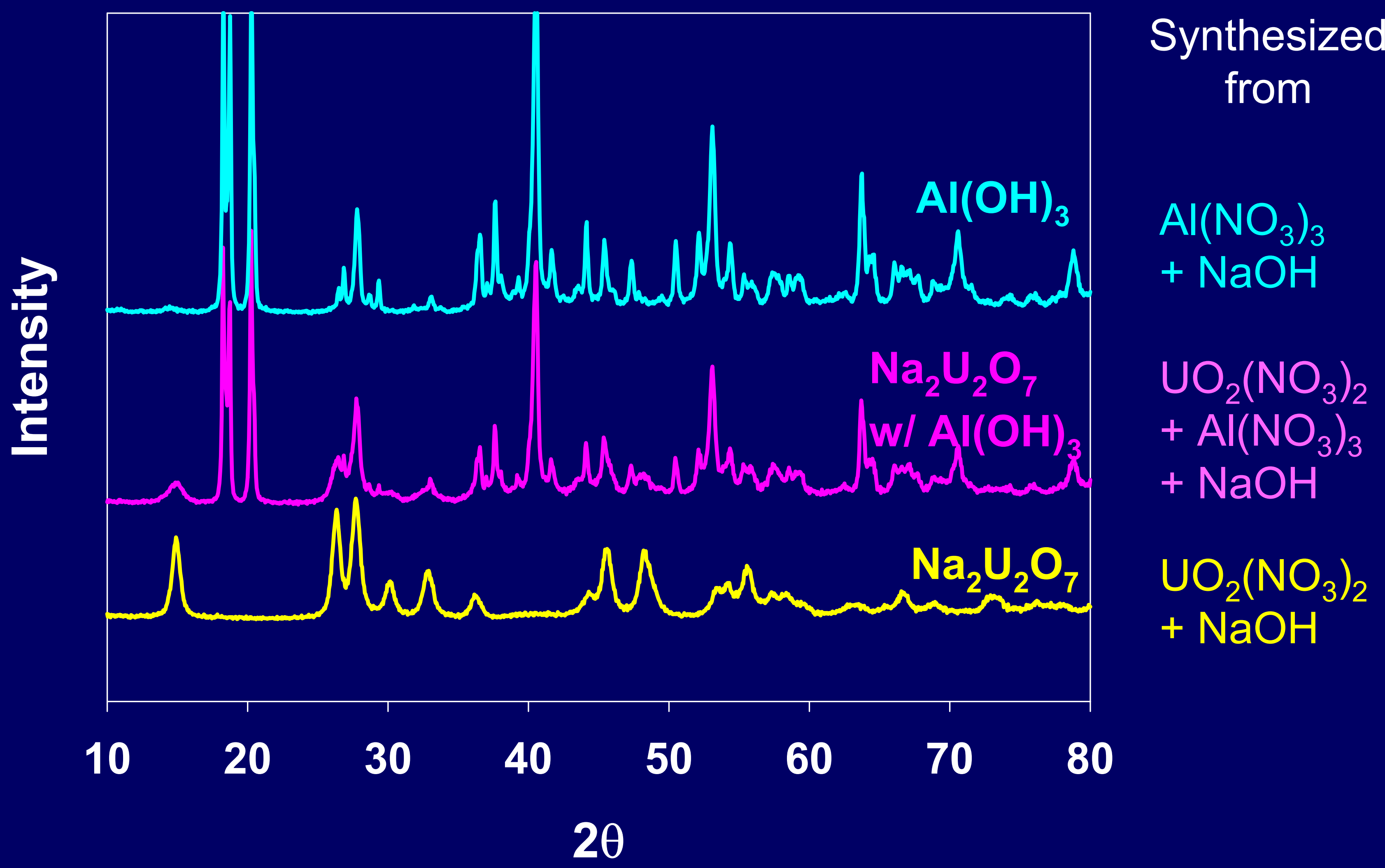

# $^{23}Na$ MAS NMR

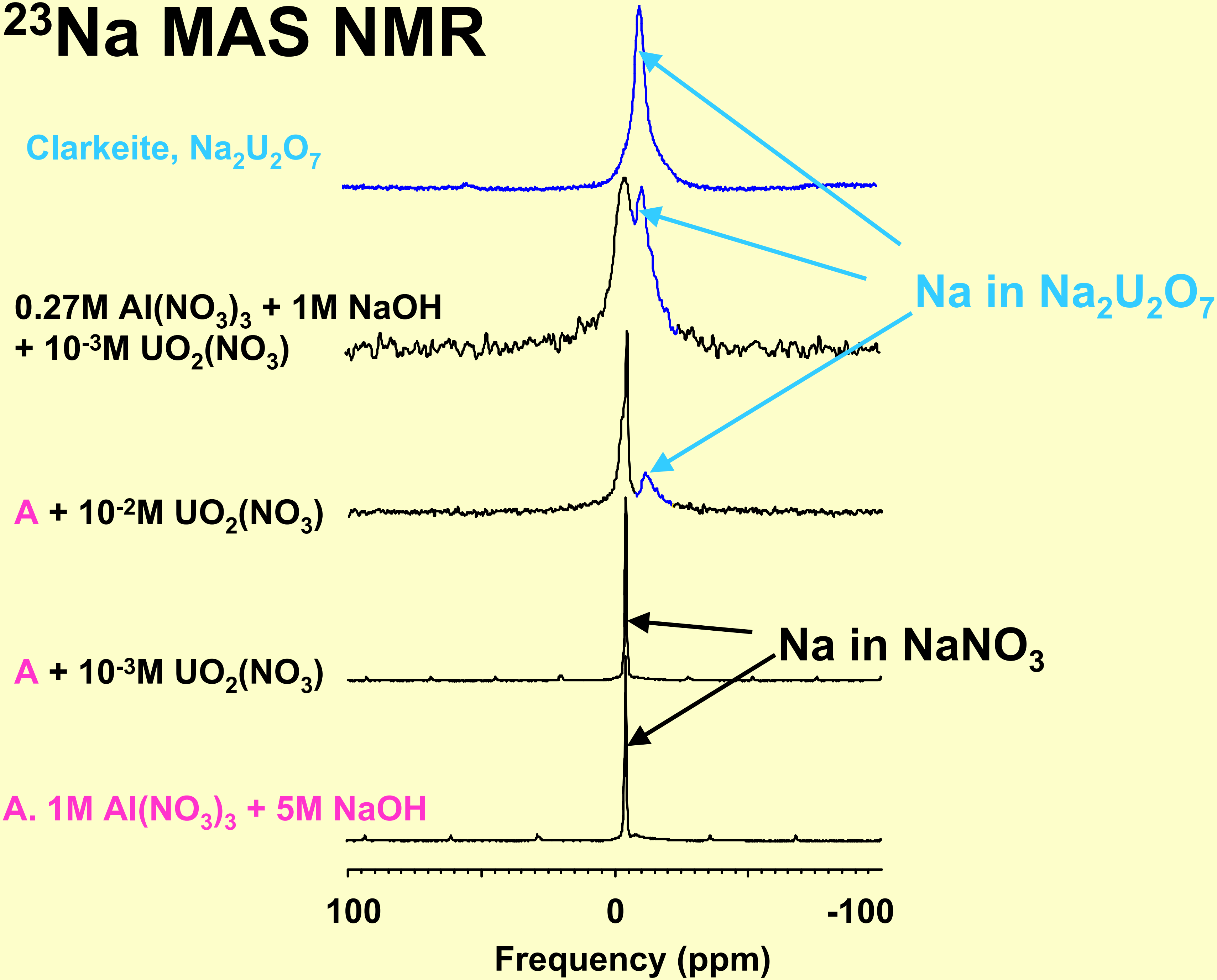

Clarkeite, Na2U2O7
0.27M Al(NO3)3 + 1M NaOH
+ 10-3M UO2(NO3)
A + 10-2M UO2(NO3)
A + 10-3M UO2(NO3)
A. 1M Al(NO3)3 + 5M NaOH
Na in Na2U2O7
Na in NaNO3
100
0
-100
Frequency (ppm)

# Uranium EXAFS and RDFs

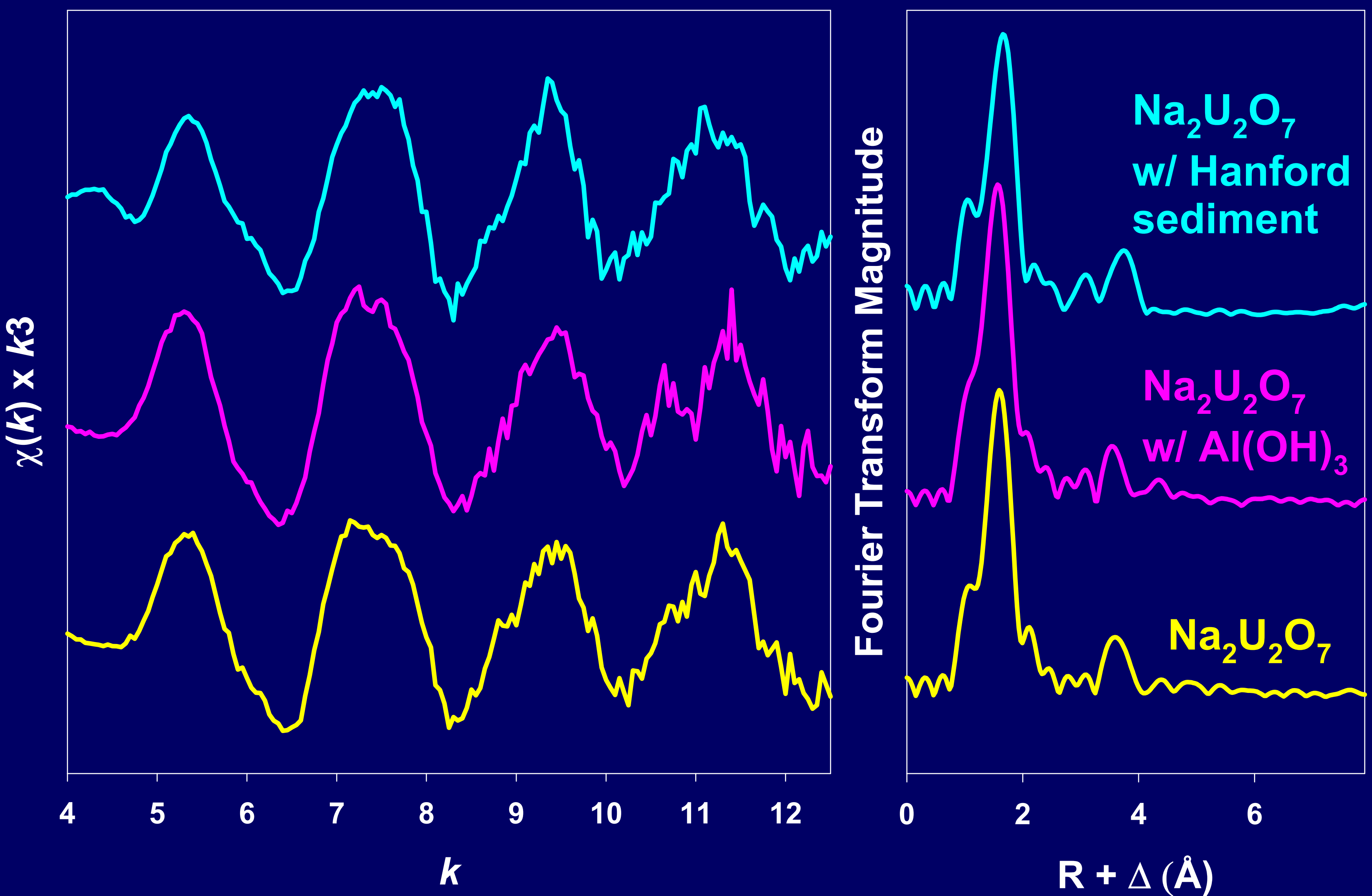

# Hypotheses

Sediments may undergo immediate dissolution as leaking hyperalkaline and saline fluid enters the vadose zone

Aluminum may inhibit dissolution

There is a strong potential for *in situ* formation of aluminosilicates, e.g., feldspathoids and zeolites

# Changes in Si concentration with time and Al concentration in the soil solution

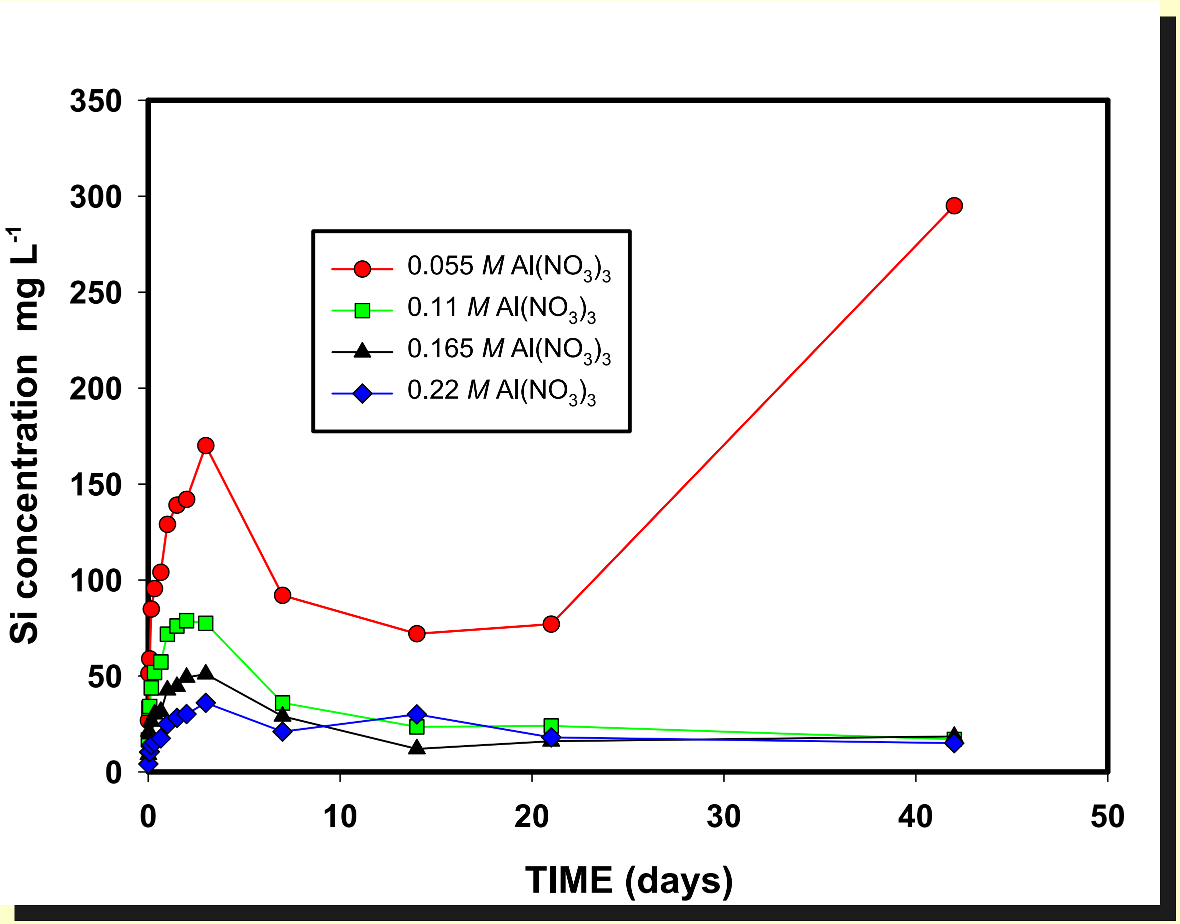

# Changes in Fe concentration with time and Al concentration in the soil solution

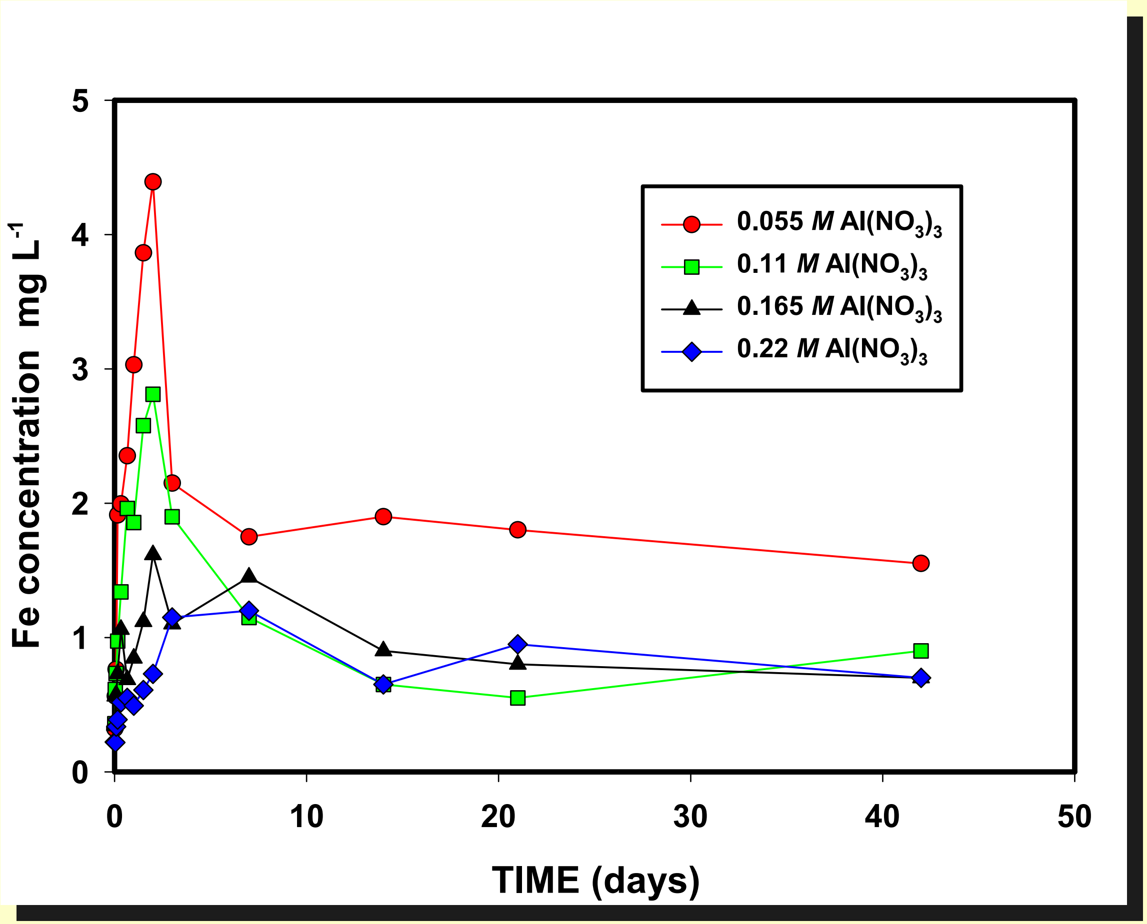

# Changes in K concentration with time and Al concentration in the soil solution

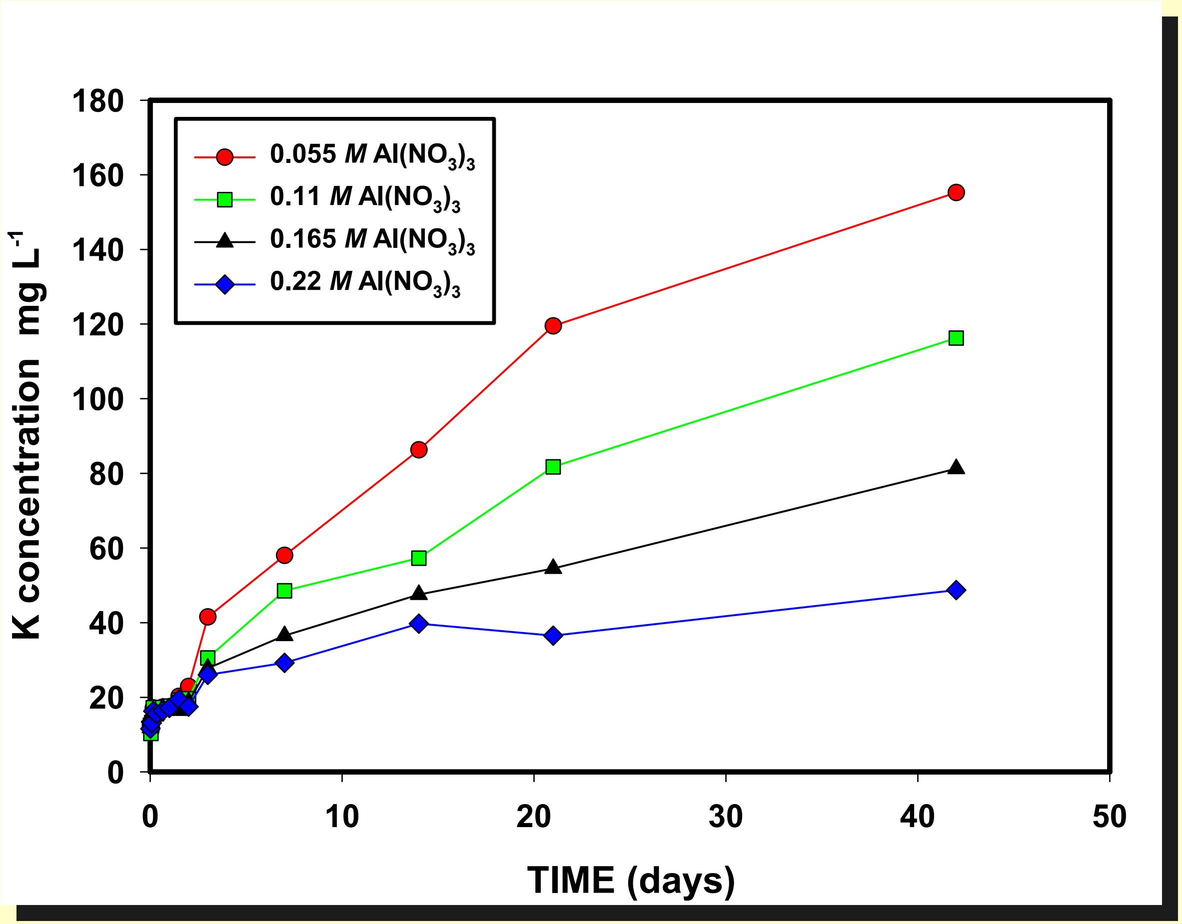

# Changes in Al concentration with time and Al concentration in the soil solution

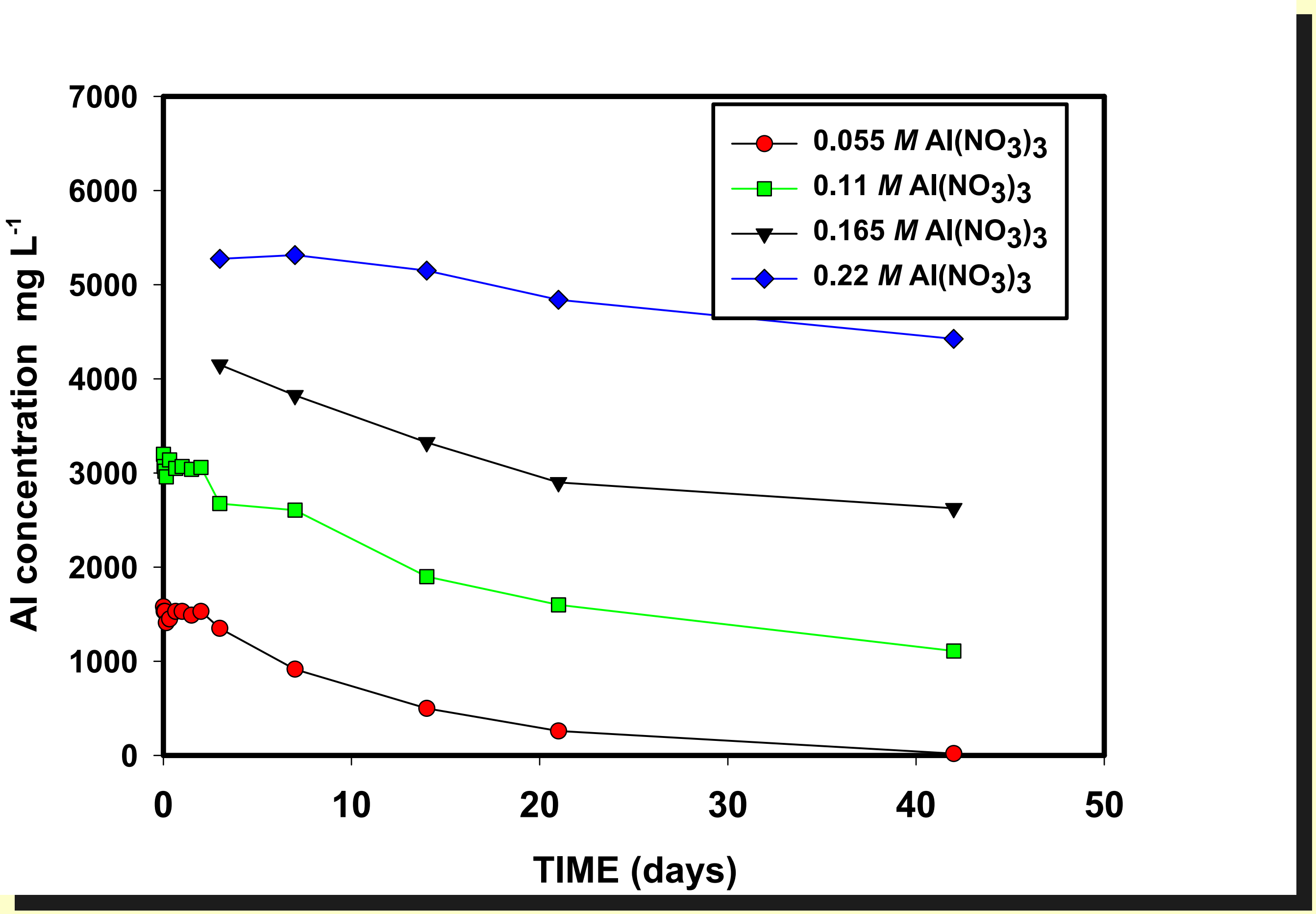

# Cr at the Hanford site

Cr(VI) in the form of potassium dichromate was used as an oxidant in the REDOX process to manipulate the valence state of Pu and U

The residual Cr(VI) was discharged to S-SX tanks

The estimated Cr concentration at the time of the leak(s) ranged from 0.0509 to 0.413 mol $L^{-1}$

The estimated total mass of Cr(VI) loss to the vadose zone from S/SX tanks is 2,685 kg (Jones et al, 2000), and Cr(VI) is considered the most significant contaminant at Hanford (Serne et al., 2001)

# Cr: laboratory studies

- Cr(VI) can be reduced homogeneously by dissolved Fe(II) or by structural Fe(II) in minerals.

- Past studies: Peterson et al (1997) on magnetite, Patterson and Fendorf (1997) on iron sulfide, Eary and Rai (1988) and Ilton and Veblen (1994) on biotite.

## *Homogeneous Cr(VI) reduction*

$Cr(VI)_{(aq)} + Fe(II)_{(aq)} = Cr(V) + Fe(III)$

$Cr(V)_{(aq)} + Fe(II)_{(aq)} = Cr(IV) + Fe(III)$

$Cr(IV)_{(aq)} + Fe(II)_{(aq)} = Cr(III) + Fe(III)$

Overall: $Cr(VI)_{(aq)} + 3Fe(II)_{(aq)} = Cr(III) + 3Fe(III)$

$Cr(III) + Fe(III) + 3OH^{-} \rightarrow (Cr,Fe)_2O_3(s) + FeO(OH)(s)$

$Cr(III) + Fe(III) + 3OH^{-} \rightarrow (Cr_xFe_{1-x})(OH)_3(s)$

# *Homogenous Cr(VI) reduction*

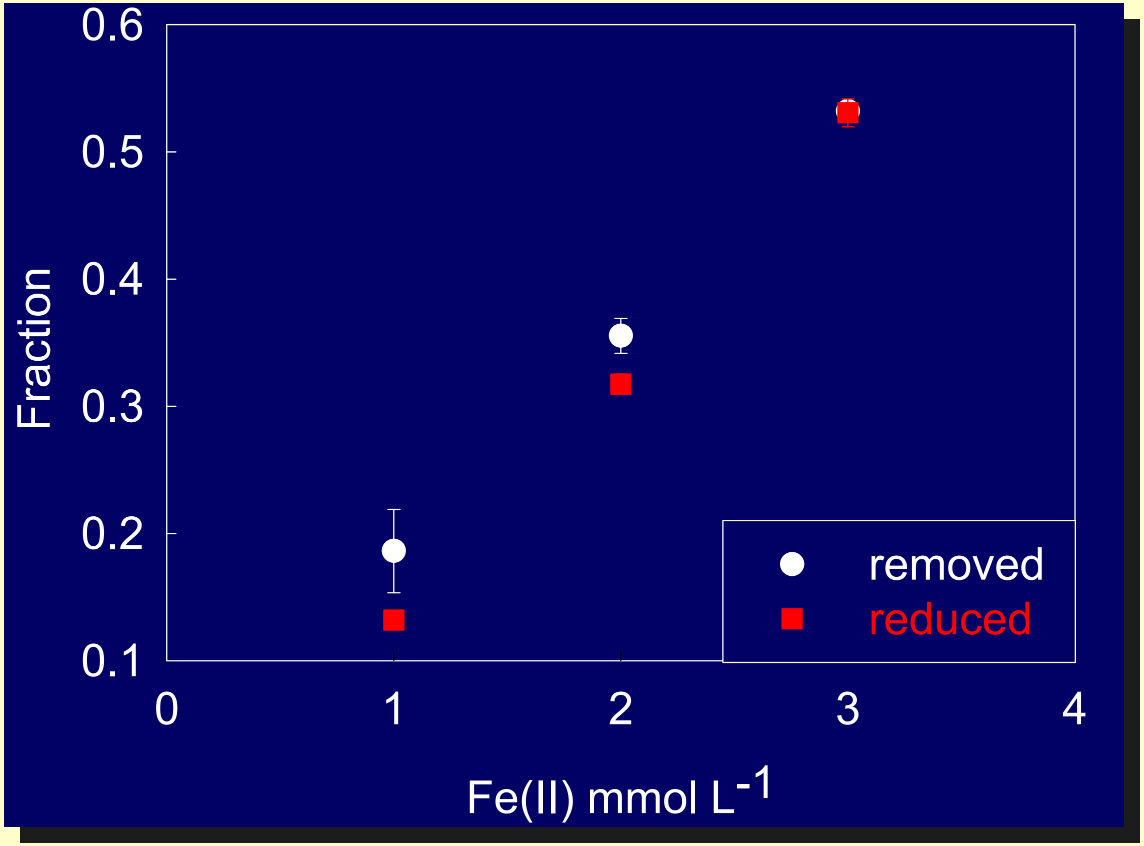


- pH 13.5
- Instantaneous
- Red-brown precipitates
- Cr/Fe follows 1:3 ratio but reduction of all the Cr was not observed

# *Homogeneous Cr(VI) reduction: XRD of reaction products*

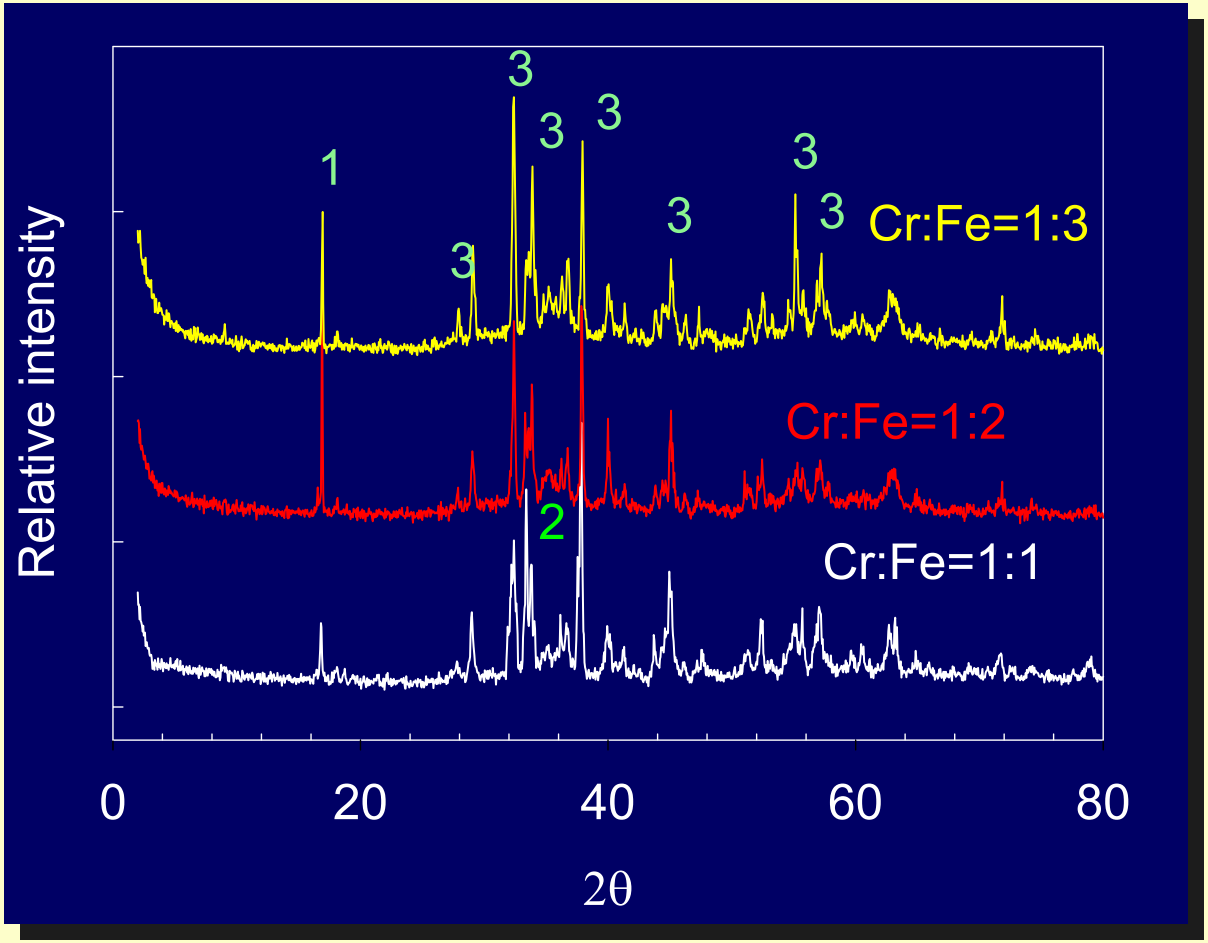


1. Akaganeite FeO(OH)
2. Iron chromium oxide $(Fe_{0.6}Cr_{0.4})_2O_3$
3. Iron oxide hydroxide FeO(OH)

## *Cr removed from solution by reaction with biotite in the presence of 2 M NaOH*

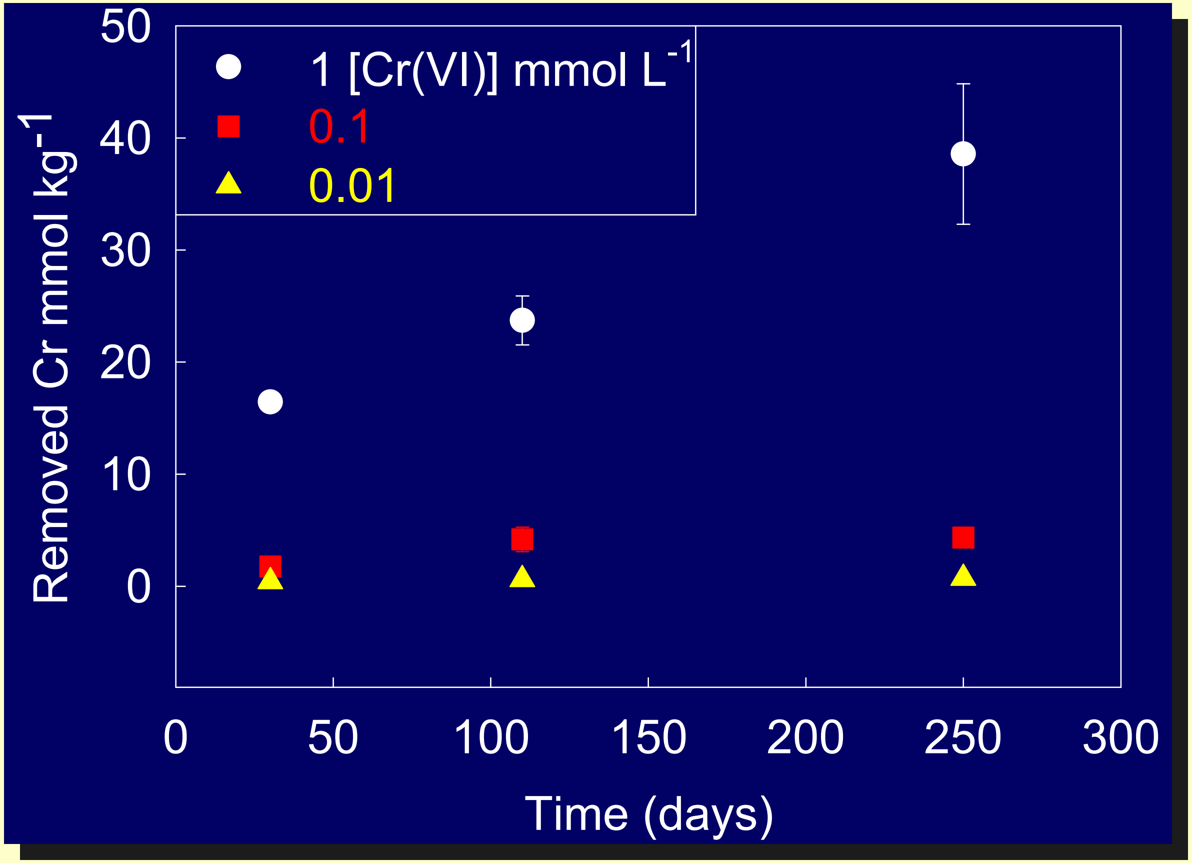


T = 50°C

# X-ray Absorption Near-edge Structure (XANES) Spectroscopy

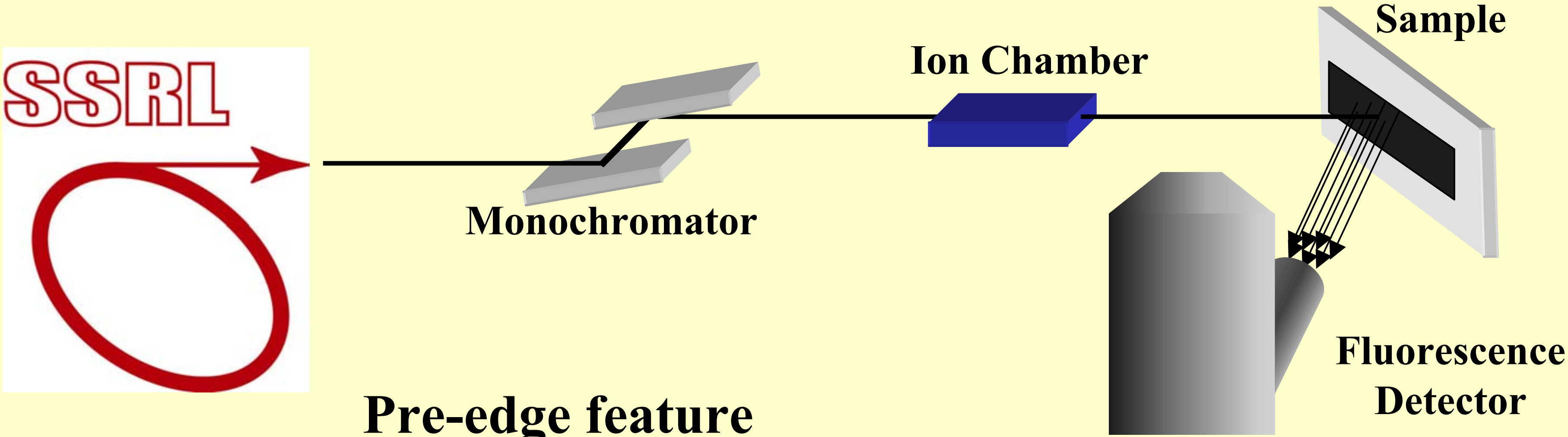


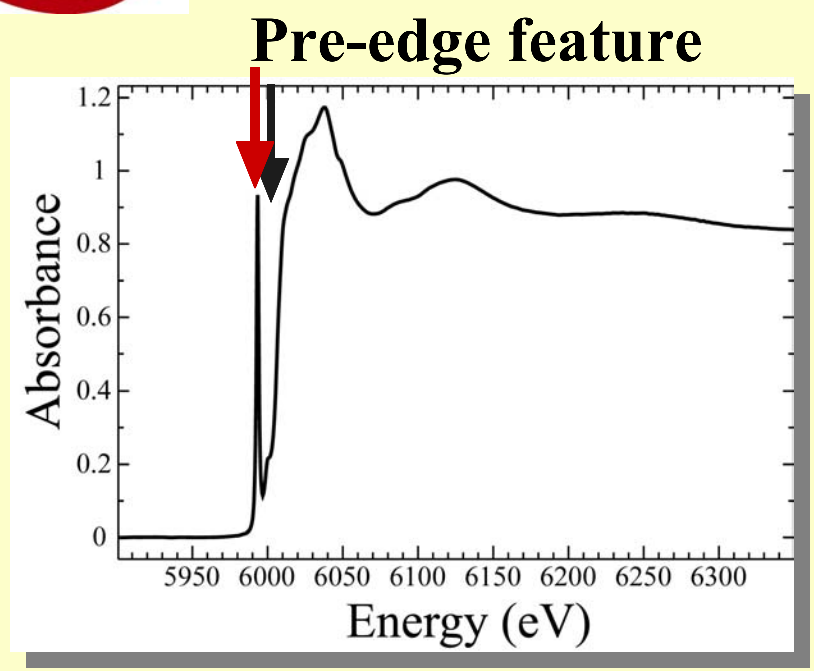

# Beamline Specific Calibration of Cr Oxidation State 1. Spectra of Mechanical Mixtures

## BL 11-2

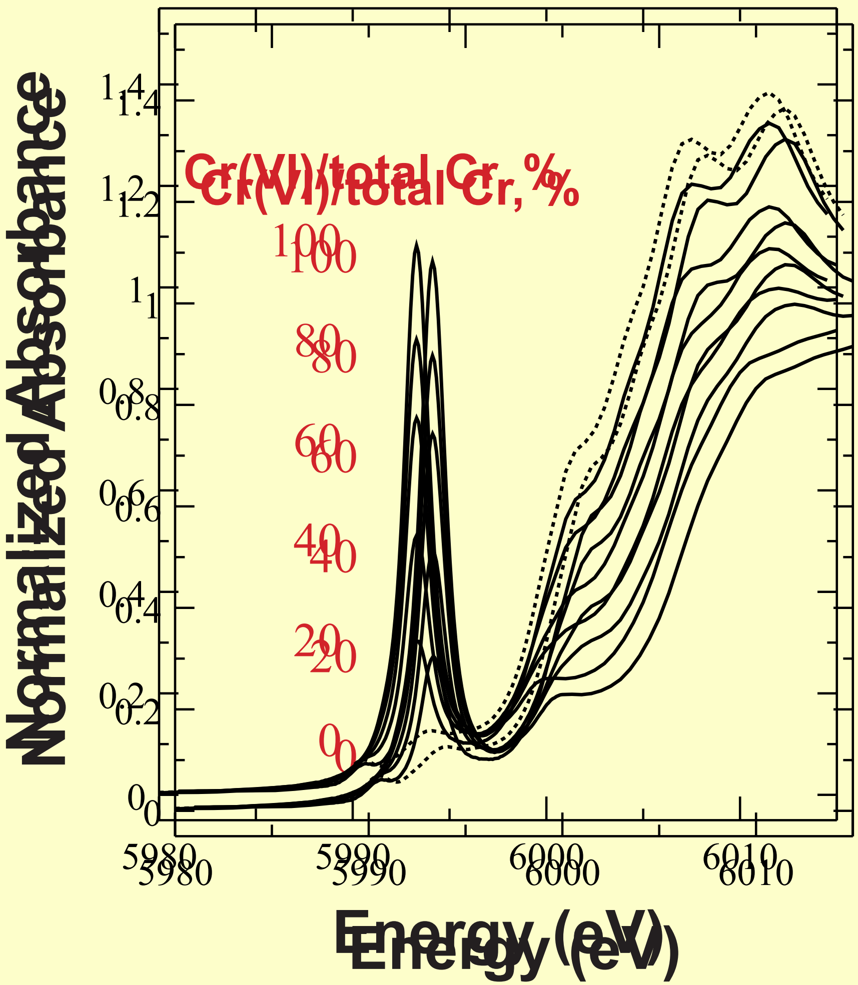


## BL 4-3

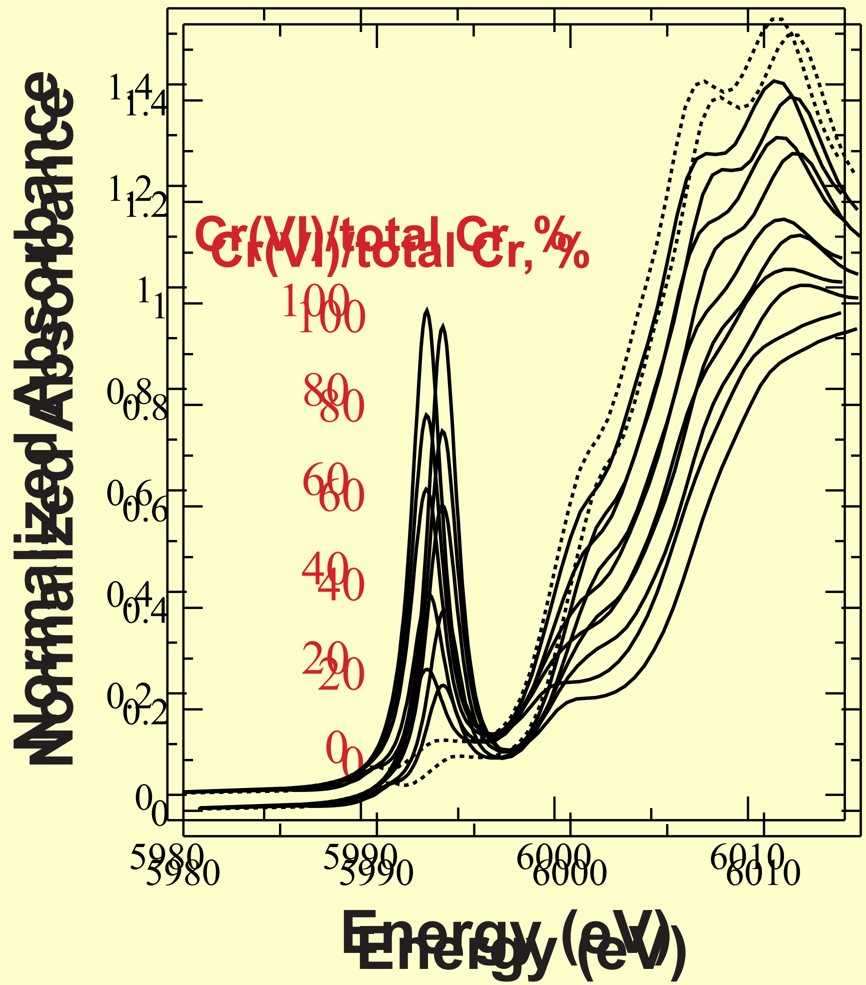

- Cr(VI) on biotite was reduced.

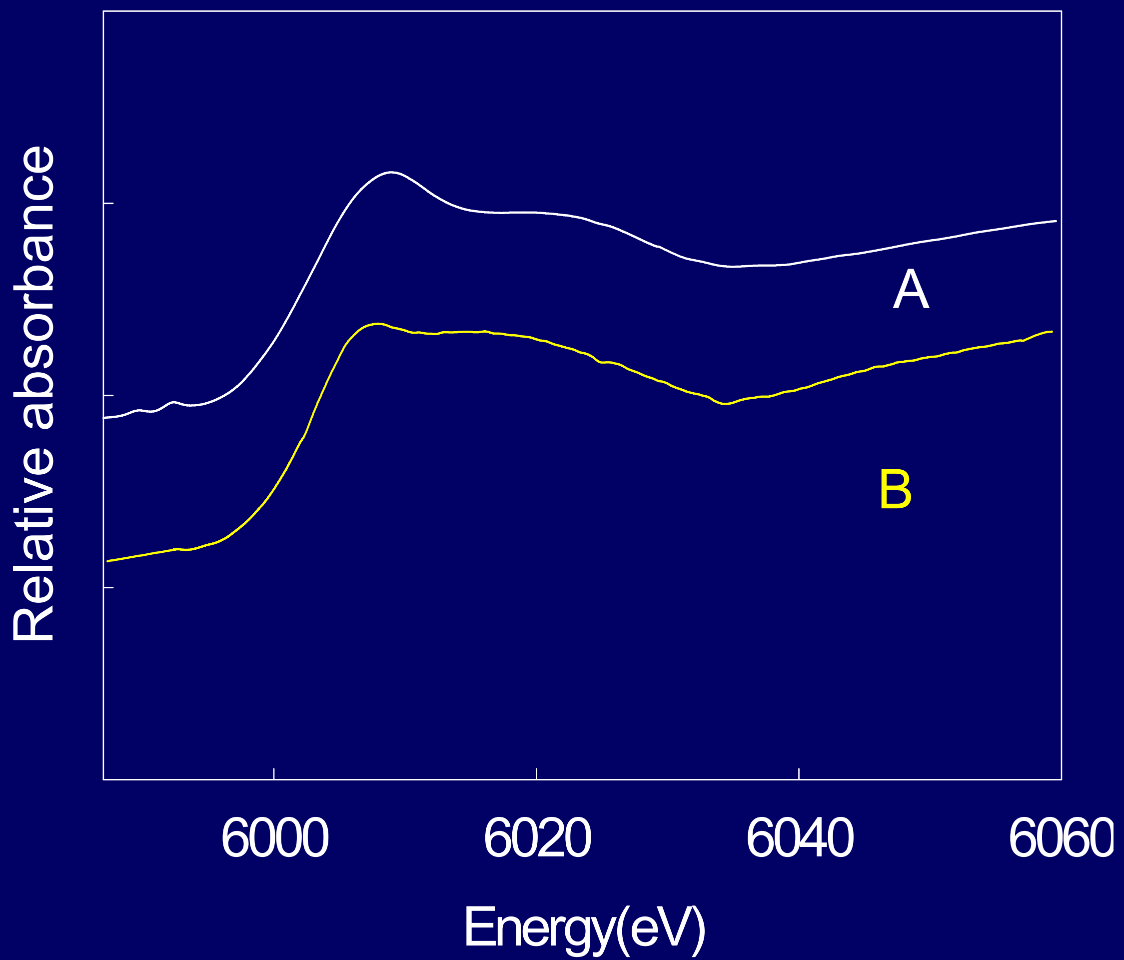

# Cr(VI) experiments, PNNL

Batch and saturated 1-D miscible displacement experiments were conducted under alkaline and high IS conditions, in a $CO_2$- and $O_2$- free environment, at 50 $^0$C

Hanford sediments were treated in batch reactors or in packed columns with Al-rich (0.055-0.165 *M*), alkaline (1-4 *M* NaOH) and saline (1 *M* $NaNO_3$) solutions considered to be representatives of the REDOX tank wastes

Cr(VI) concentration in the leaching solutions was 0.192 and 1.923 m*M*

## Changes in Cr(VI) concentration during leaching first with the $Na_2CrO_4$ solution, and then with the alkaline solution (4.08 h)

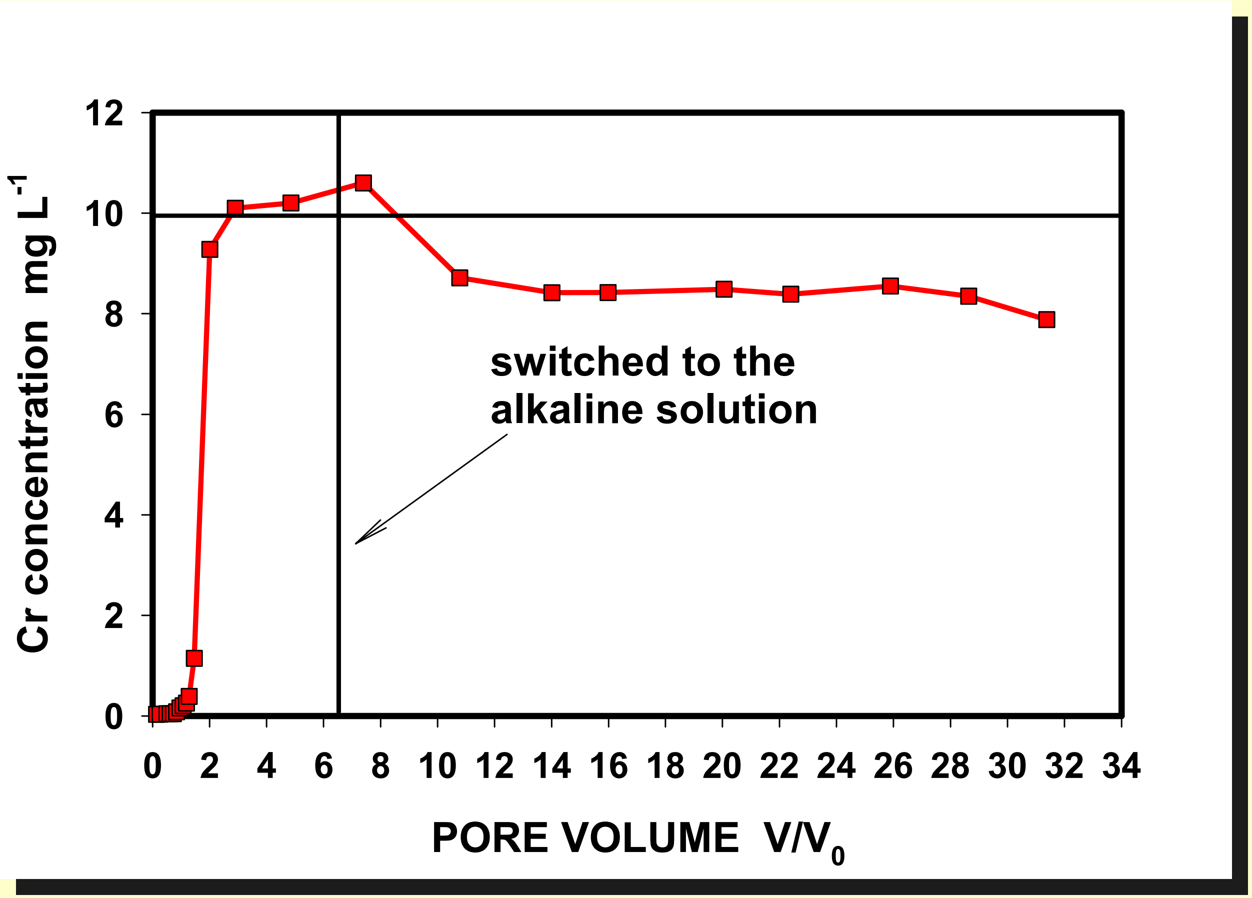

# Cr attenuation (8.05 h) Leaching solution: 1*M* NaOH, 1*M* $NaNO_3$, 0.055 *M* $Al(NO_3)_3$, 0.192 m*M* Cr as $Na_2CrO_4$

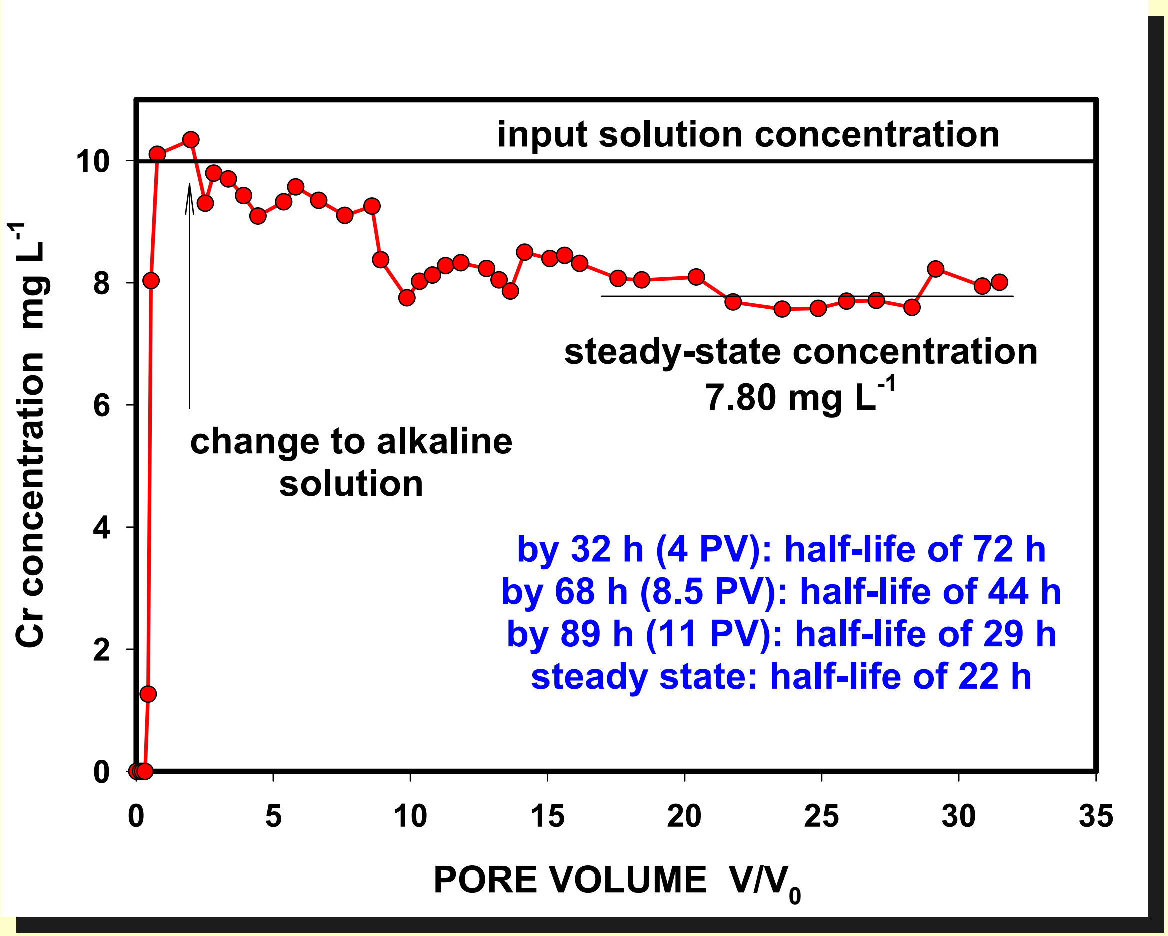

# Cr attenuation (32.5 h) Leaching solution: 1*M* NaOH, 1*M* $NaNO_3$, 0.055 *M* $Al(NO_3)_3$, 0.192 m*M* Cr as $Na_2CrO_4$

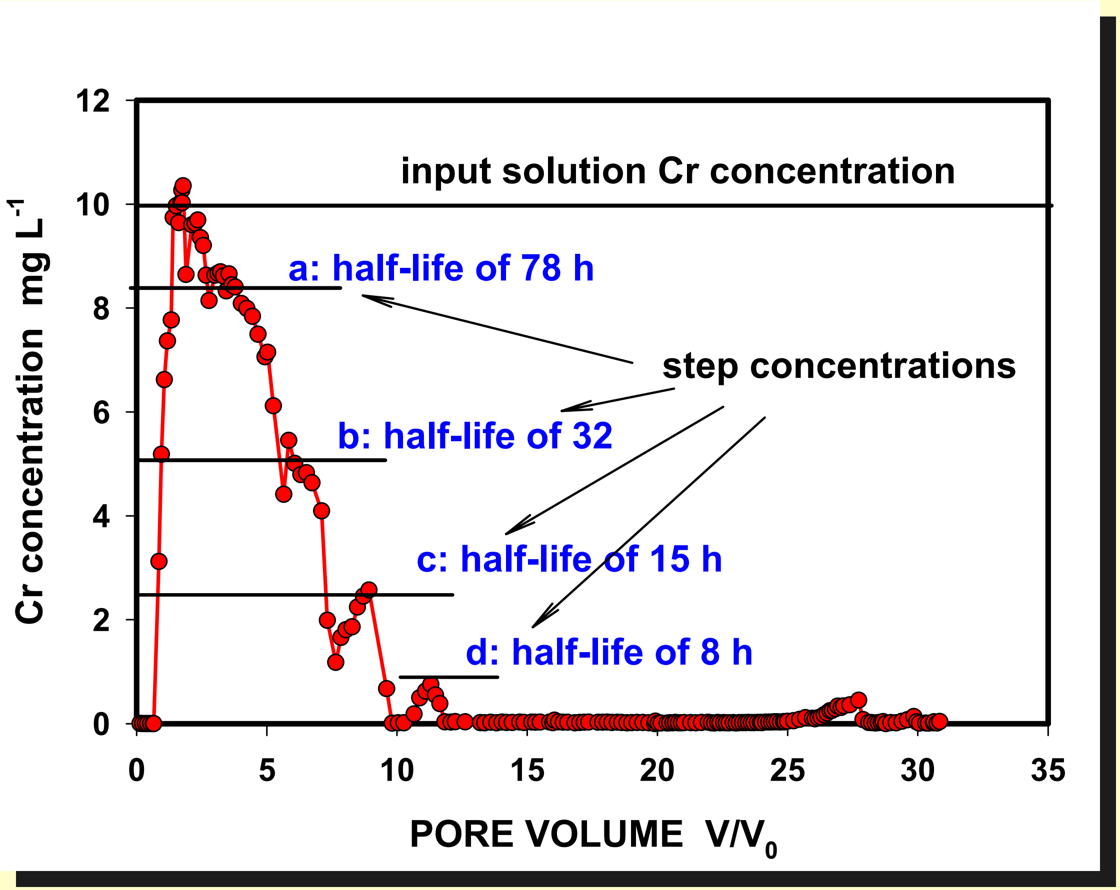

# Stop-flow Cr(VI) leaching (8.53 h): 1*M* NaOH, 1*M* $NaNO_3$, 0.055 *M* $Al(NO_3)_3$, 0.192 m*M* Cr as $Na_2CrO_4$

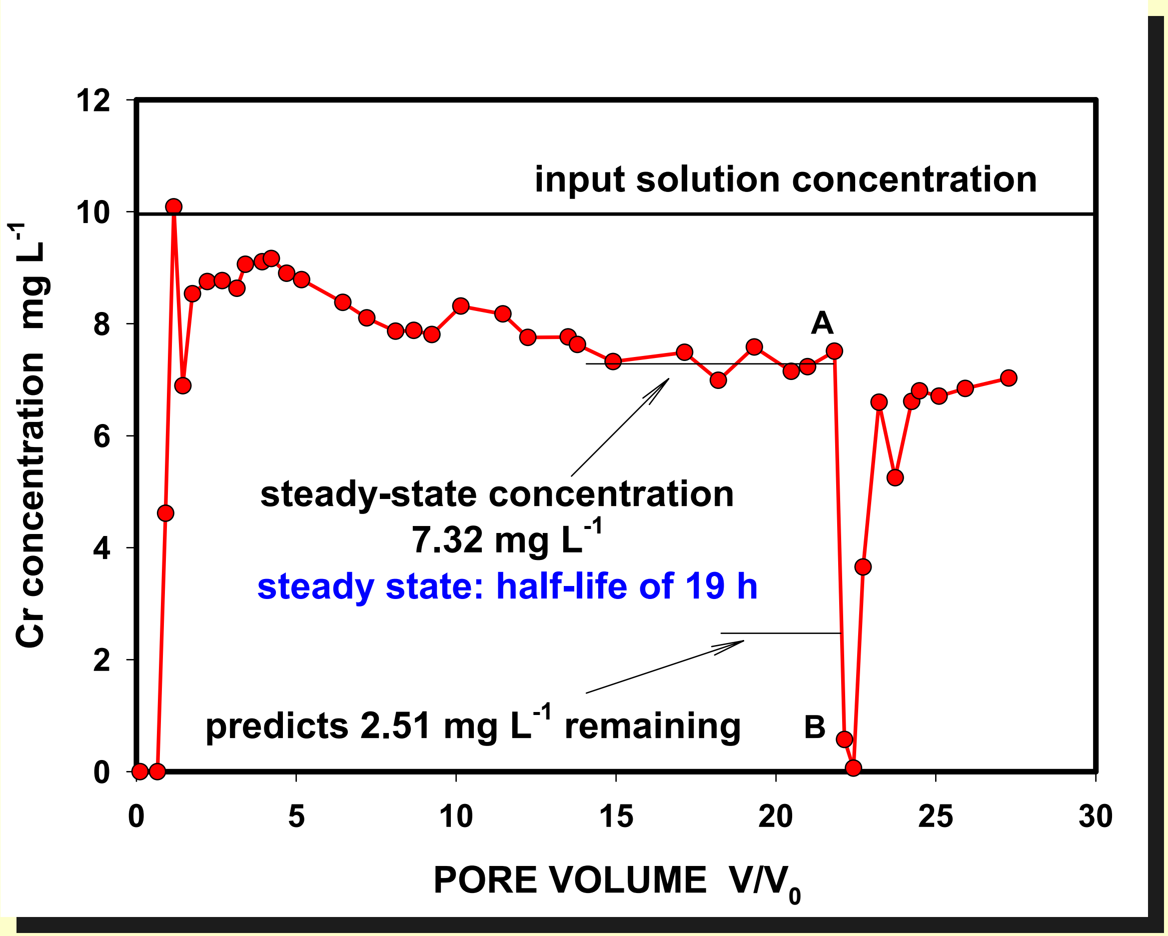

# Stop-flow Si, K, and Fe release - Leaching solution: 1*M* NaOH, 1*M* $NaNO_3$, 0.055 *M* $Al(NO_3)_3$, 0.192 m*M* Cr as $Na_2CrO_4$

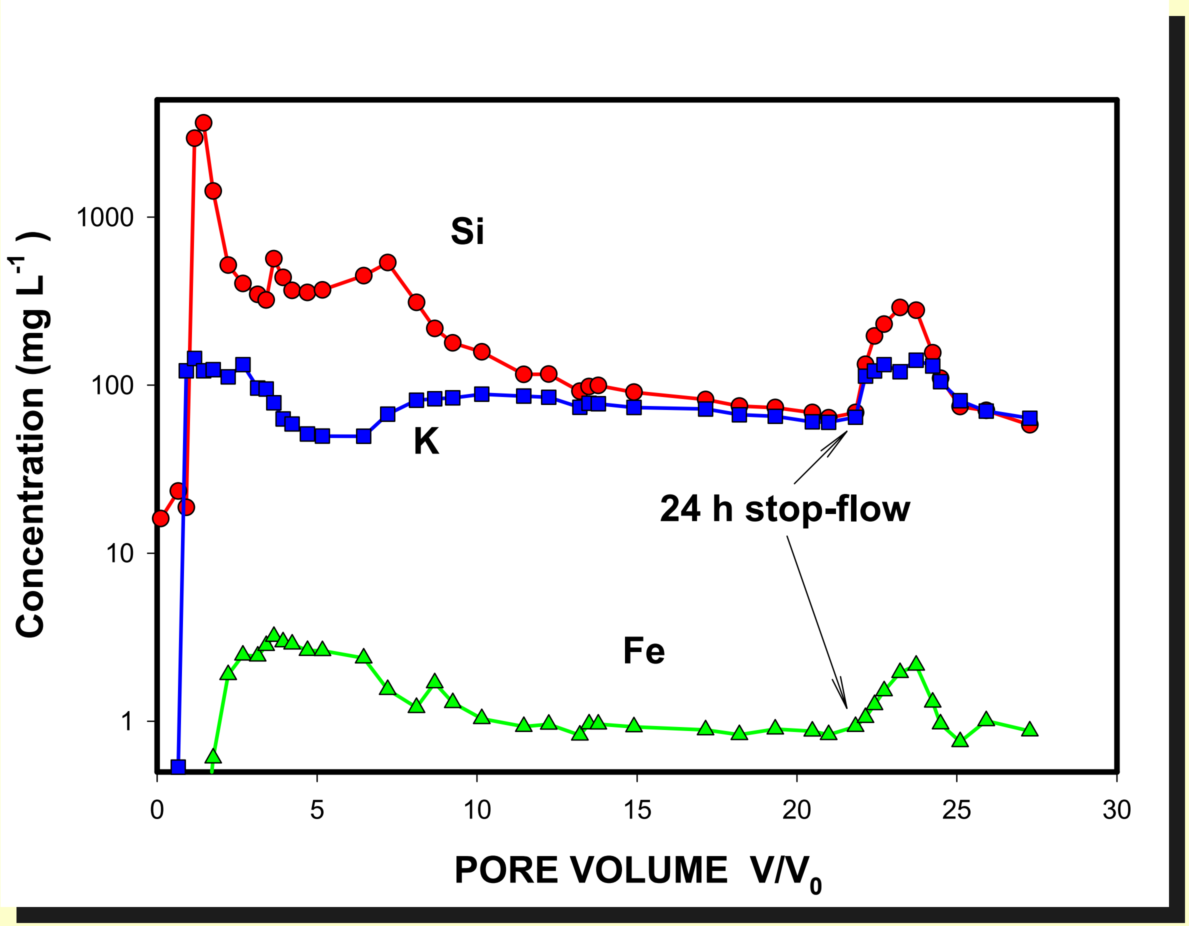

# Effect of OH on Fe release - Leaching solution: 1*M* and 4*M* NaOH, 1*M* $NaNO_3$, 0.055 *M* $Al(NO_3)_3$, 0.192 m*M* Cr as $Na_2CrO_4$

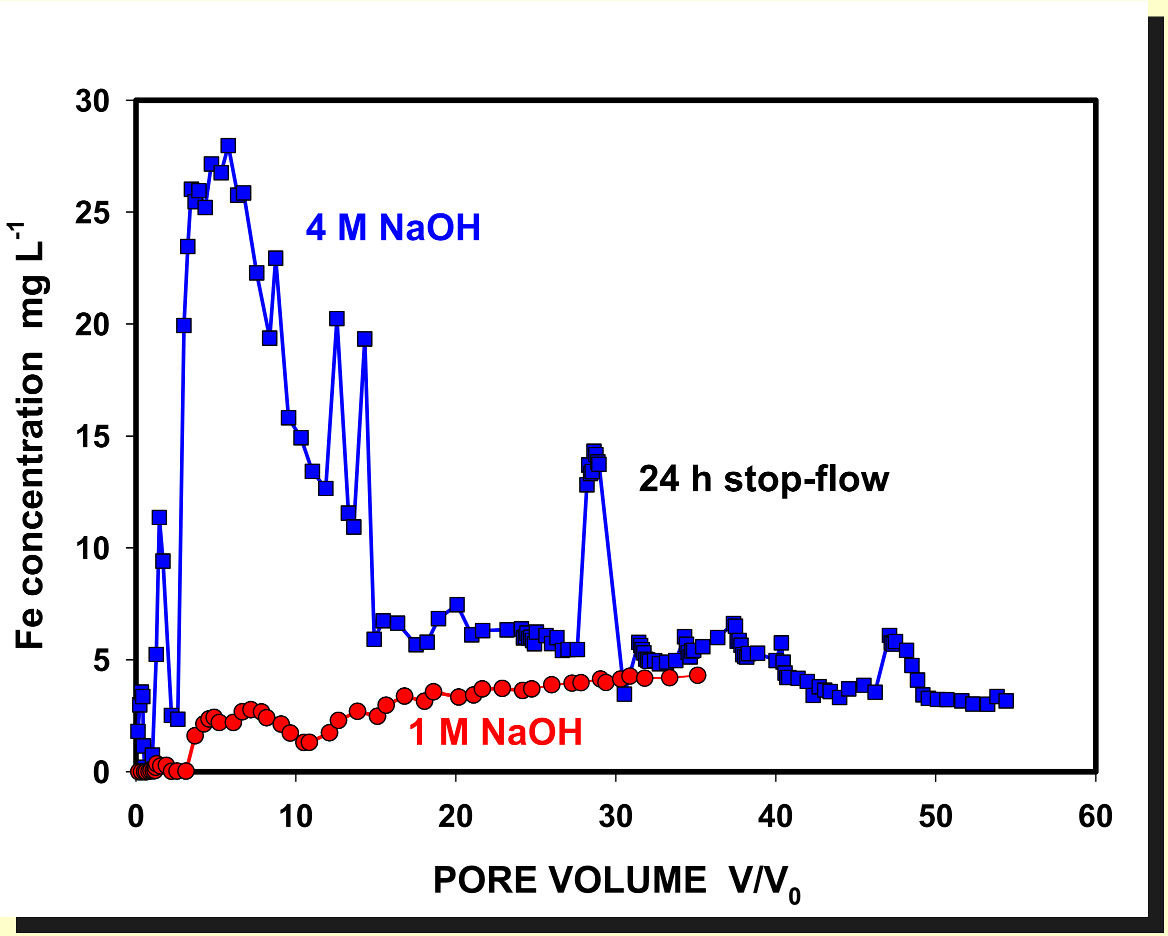

# Cr XANES - Leaching solution: 1*M* NaOH, 1*M* $NaNO_3$, 0.055 *M* $Al(NO_3)_3$, 1.923 m*M* Cr as $Na_2CrO_4$

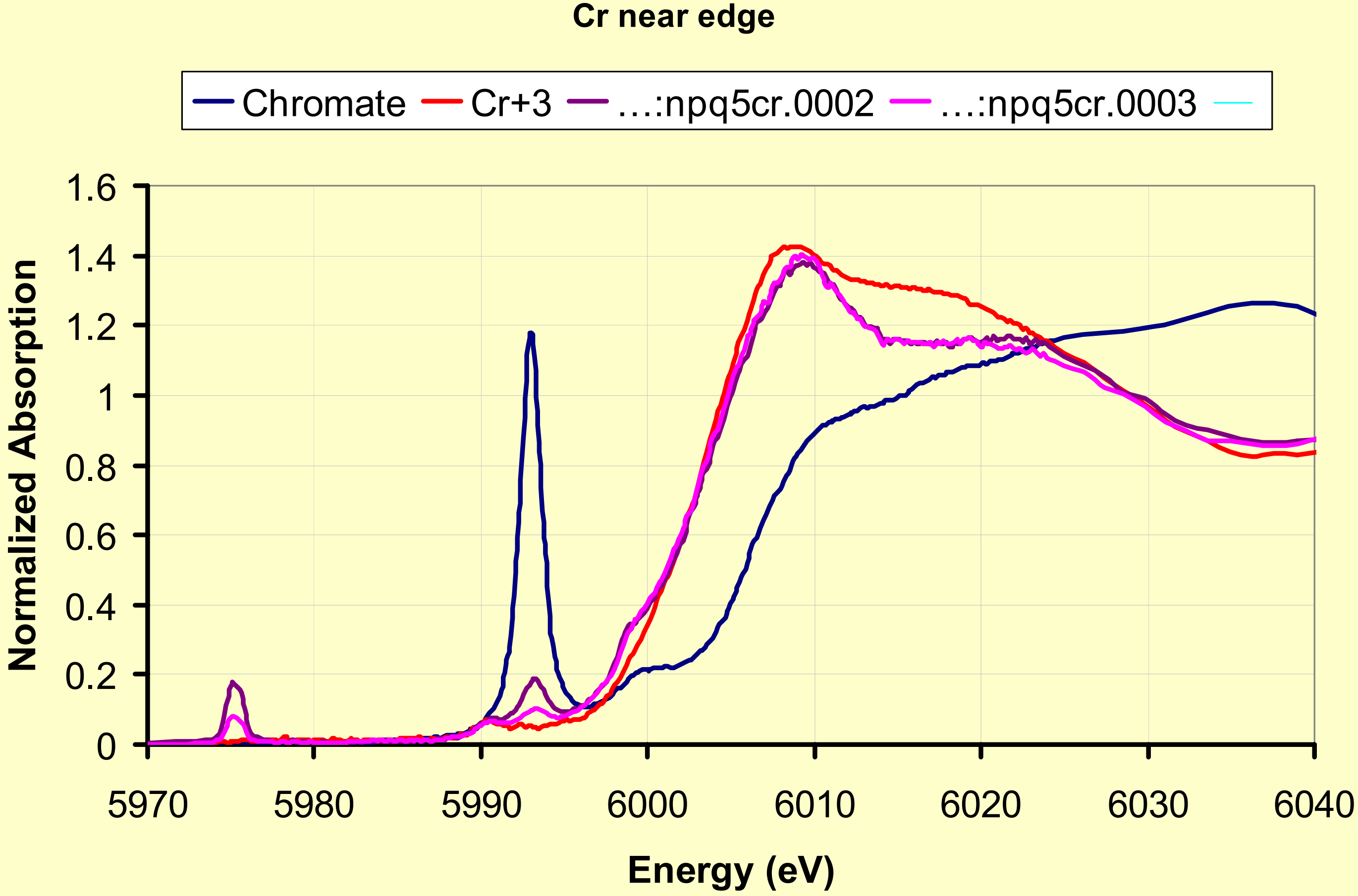

# Wide area view around the first scan region sediments from from the column leached with 100 ppm Cr(VI) solution

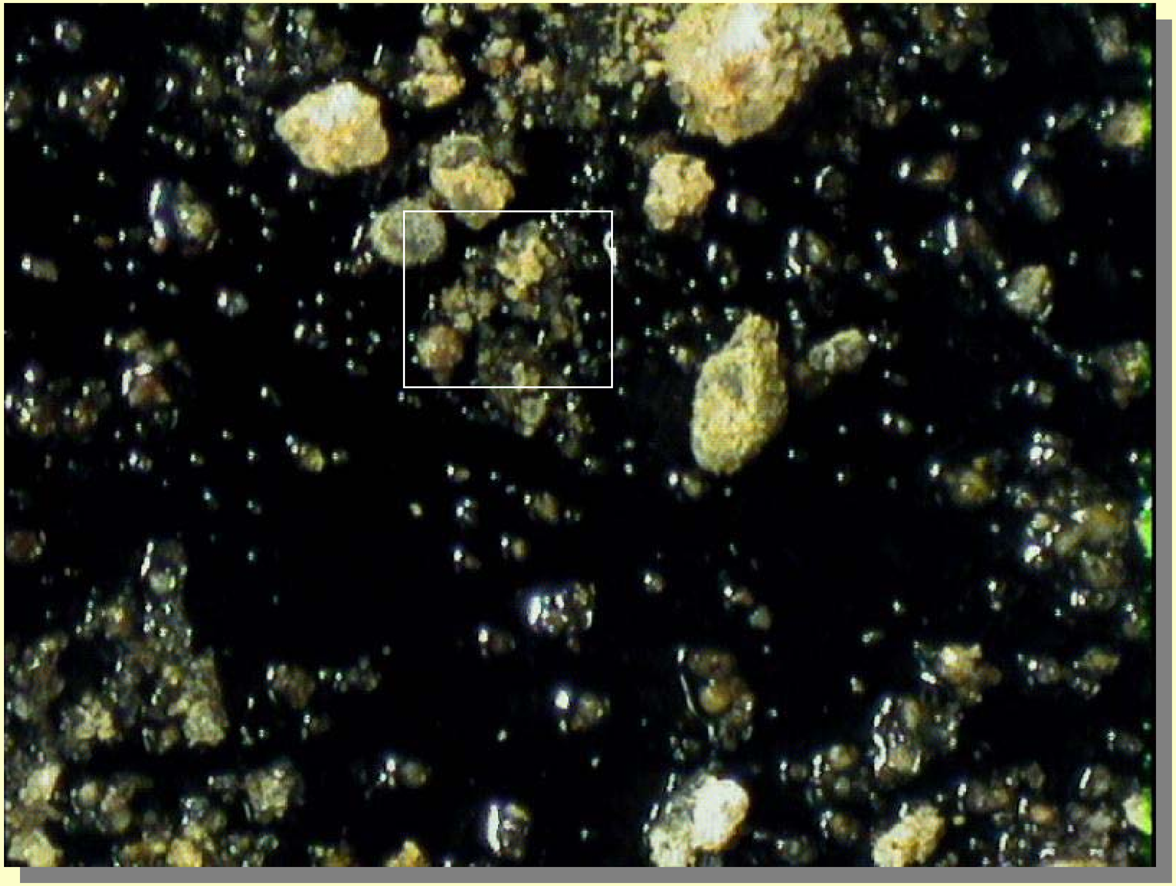

# Cr, K, and Fe elemental images 1300 x 1300 microns, 7 micron steps

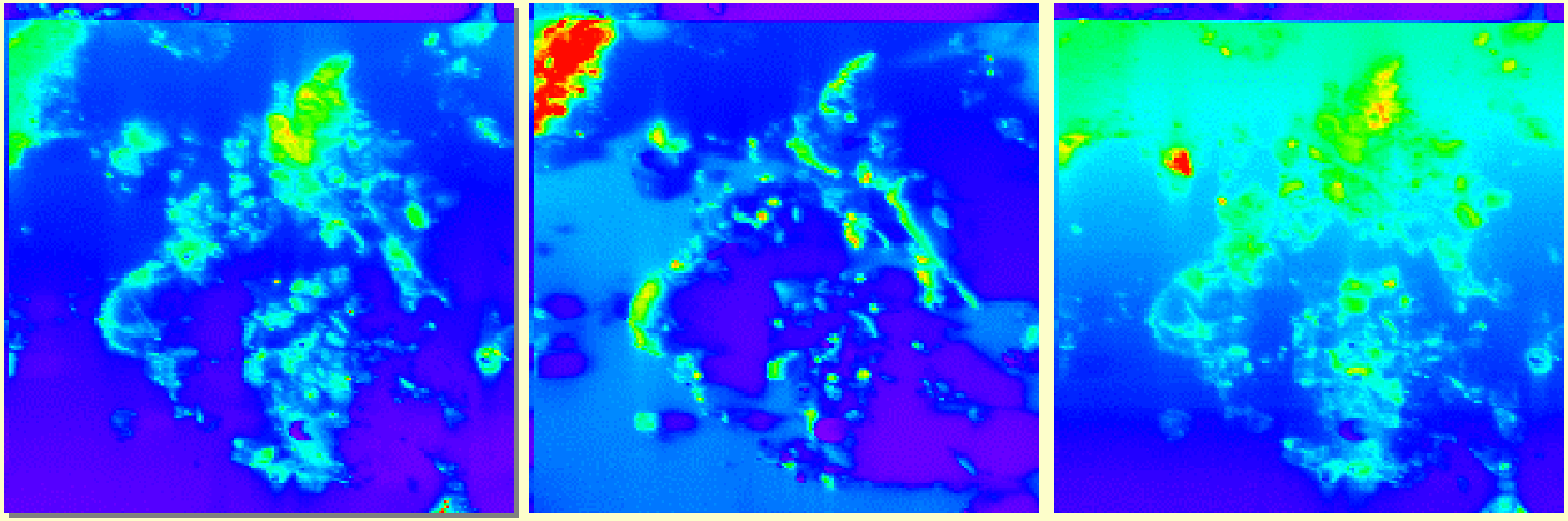

Cr K Fe

# Wide area view around the second scan region

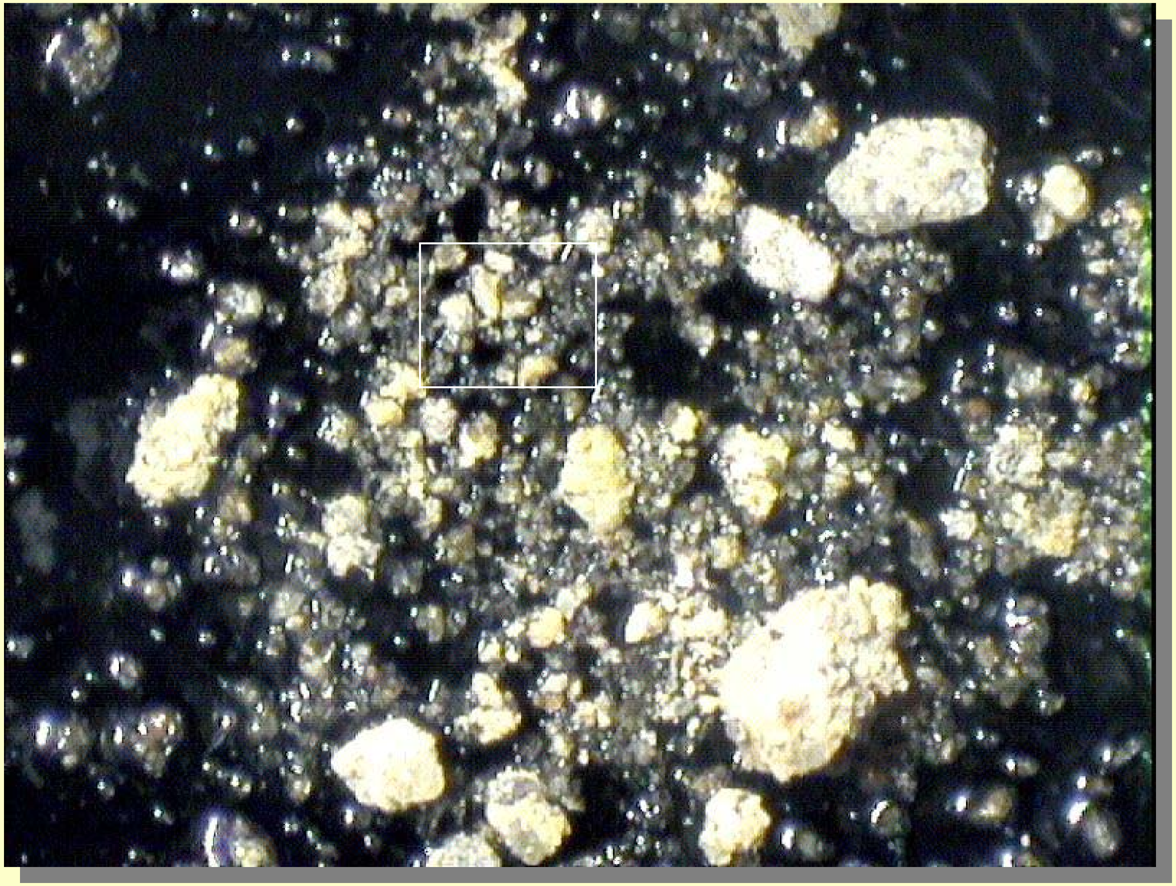

Cr, K, and Fe elemental images, 700 by 700 micron;

7 micron step size

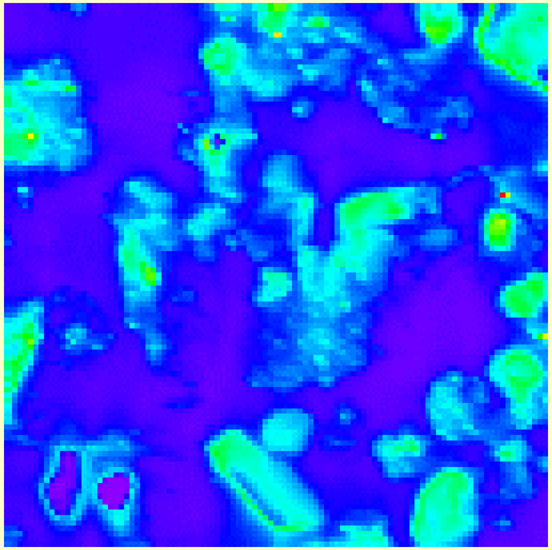

Cr

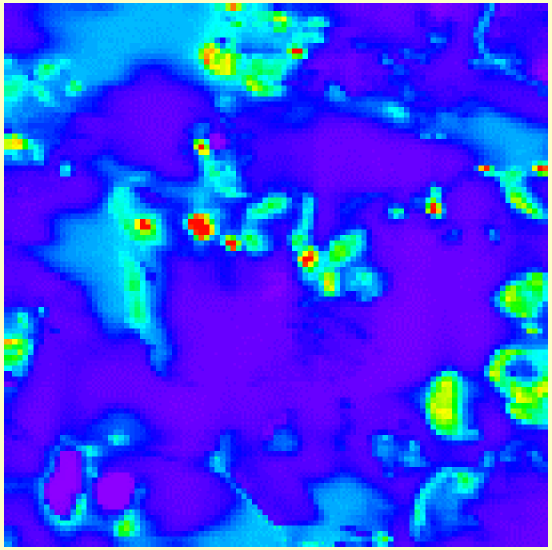

K

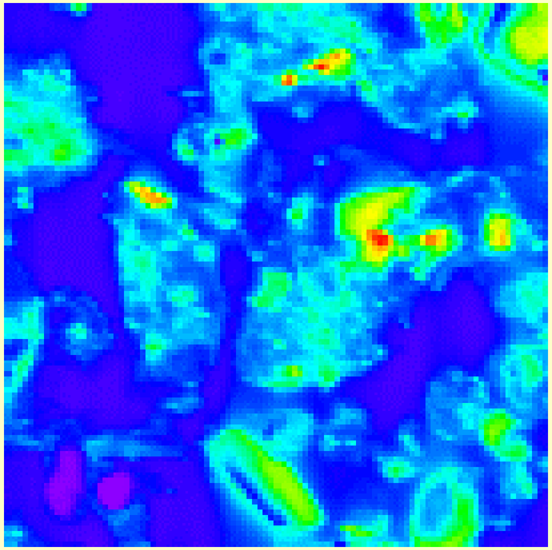

Fe

# Field Sampling

The SX Tank farm

Battelle

# Contaminated field samples from the SX Farm

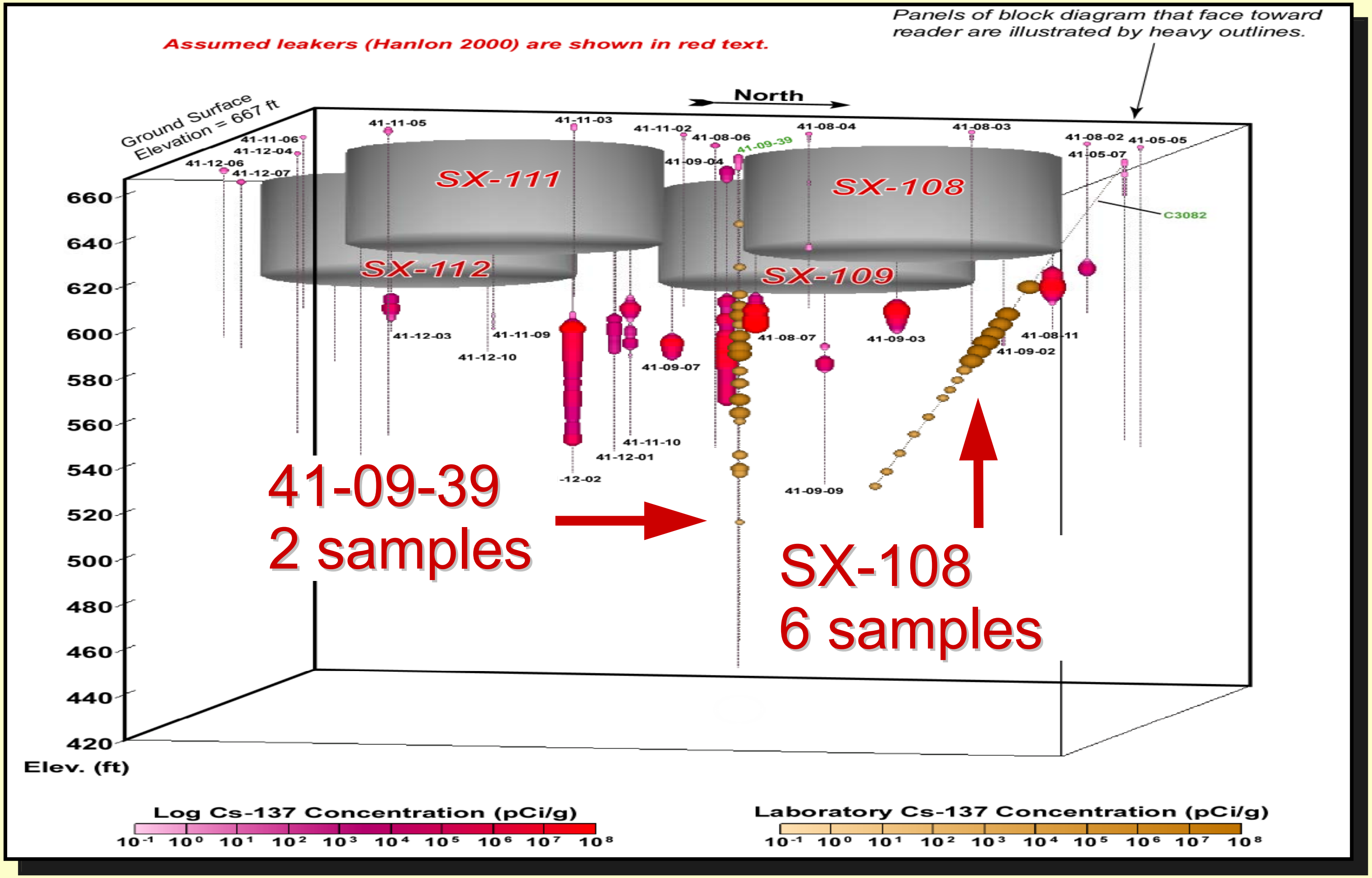

# Nature of WMA S-SX Core Samples

# SX core samples analyzed

| Sample | Depth (ft.) | Total Cr (ppm) |
|---|---|---|
| **SX-108 Core** | | |
| 6A | 80 | 955 |
| 7A | 84 | 1297 |
| 8A | 88 | 2098 |
| 9A | 92 | 1394 |
| 13A | 113 | 931 |
| 14A | 121 | 388 |
| **41-09-39 Core** | | |
| 6AB | 90 | 1186 |
| 7ABC | 83 | 2090 |

## *Cr mapping at GSE-CARS, Sector 13*

- Sediment core samples were impregnated with epoxy, cross-sectioned, polished to 0.1 mm thick and mounted onto $SiO_2$.

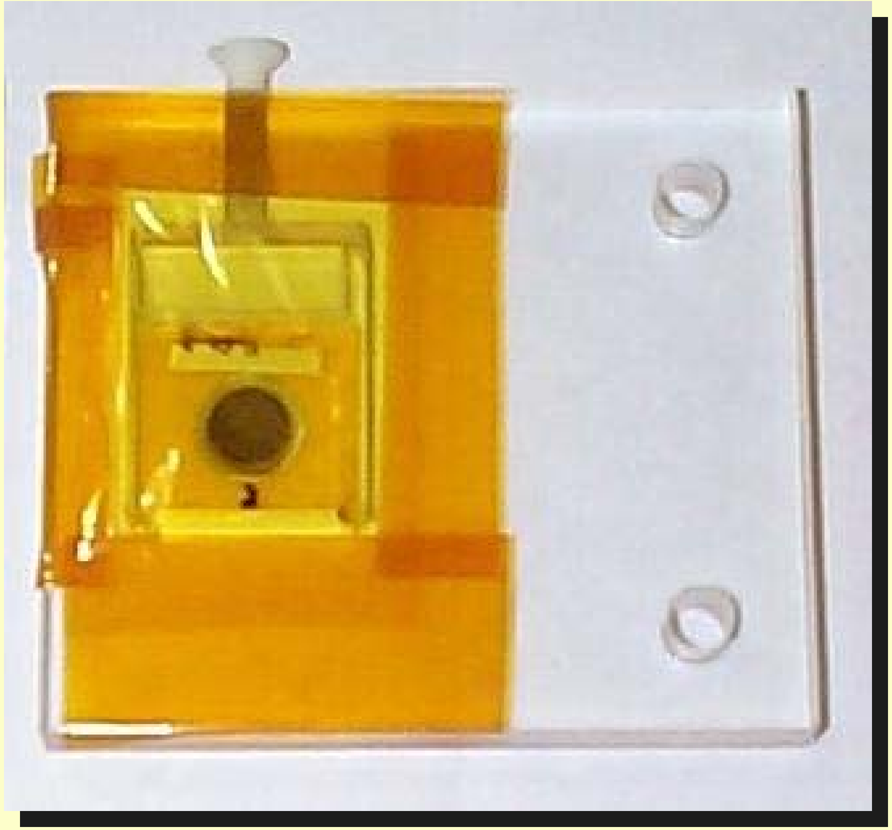

# Cr mapping at GSE-CARS, Sector 13, continued…

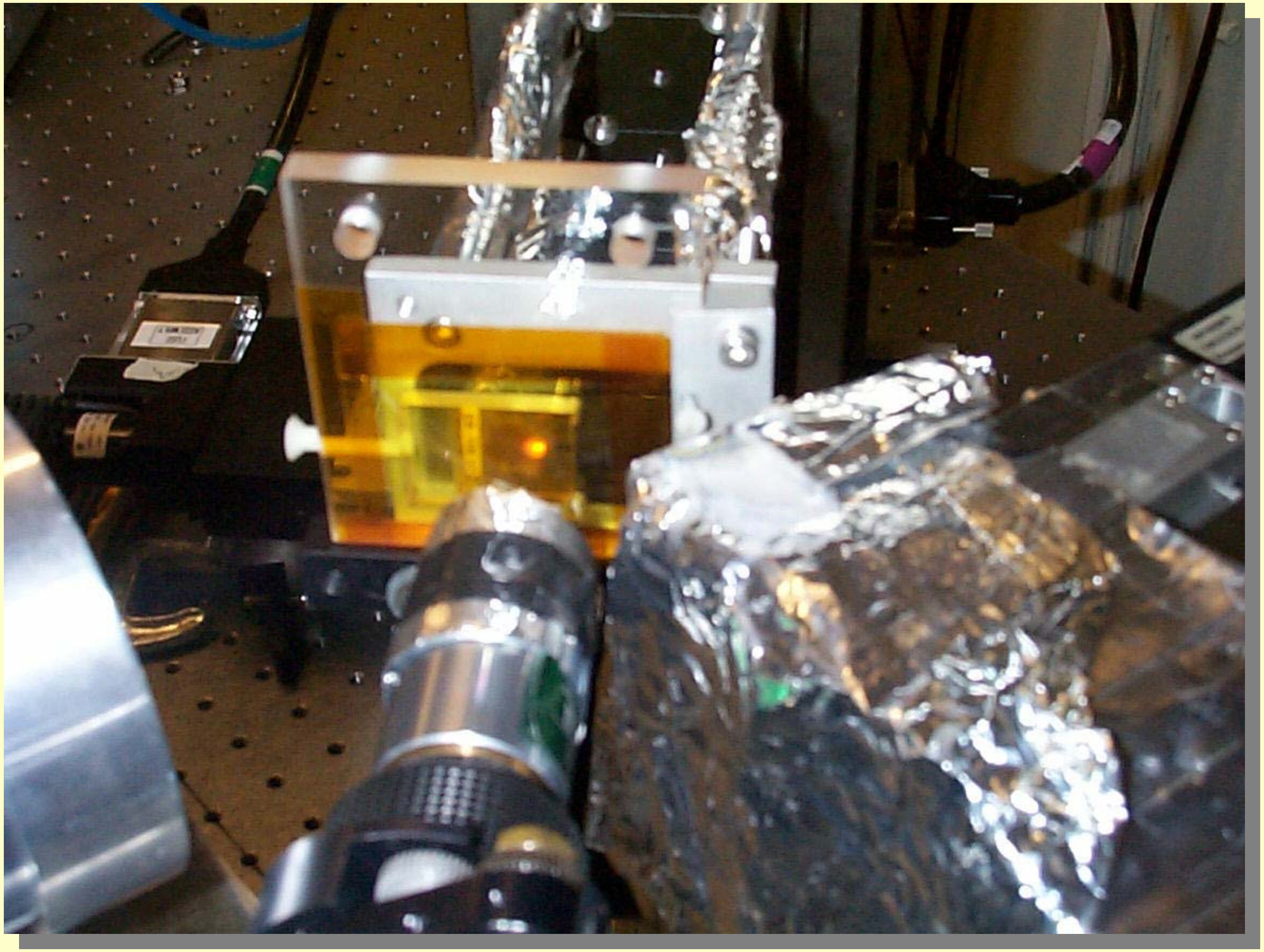

## *Element Correlation Matrix: Sample 41-09-39-6AB*

| | Ca | Cr | Fe | K | Mn | Ti |
|---|---|---|---|---|---|---|
| Ca | 1.00 | -0.30 | -0.32 | 0.65 | -0.29 | -0.22 |
| Cr | -0.30 | 1.00 | 0.81 | 0.16 | 0.94 | 0.58 |
| Fe | -0.32 | *0.81* | 1.00 | 0.16 | 0.86 | 0.54 |
| K | 0.65 | 0.16 | 0.16 | 1.00 | 0.16 | 0.23 |
| Mn | -0.29 | *0.94* | 0.86 | 0.16 | 1.00 | 0.58 |
| Ti | -0.22 | *0.58* | 0.54 | 0.23 | 0.58 | 1.00 |

## *Element Correlation Matrix: Sample SX-108-7A*

| | Ca | Cr | Fe | K | Mn | Ti |
|---|---|---|---|---|---|---|
| Ca | 1.00 | -0.16 | -0.30 | 0.75 | -0.14 | 0.03 |
| Cr | -0.16 | 1.00 | 0.53 | 0.04 | 0.56 | 0.31 |
| Fe | -0.30 | *0.53* | 1.00 | -0.14 | 0.83 | 0.24 |
| K | 0.75 | 0.04 | -0.14 | 1.00 | -0.04 | 0.33 |
| Mn | -0.14 | *0.56* | 0.83 | -0.04 | 1.00 | 0.19 |
| Ti | 0.03 | *0.31* | 0.24 | 0.34 | 0.19 | 1.00 |

# *Element Correlation Matrix: Sample SX-108-8A*

| | Ca | Cr | Fe | K | Mn | Ti |
|---|---|---|---|---|---|---|
| Ca | 1.00 | 0.31 | 0.34 | 0.38 | 0.36 | 0.31 |
| Cr | 0.31 | 1.00 | 0.59 | 0.09 | 0.60 | 0.58 |
| Fe | 0.34 | *0.59* | 1.00 | 0.11 | 0.90 | 0.54 |
| K | 0.38 | 0.09 | 0.11 | 1.00 | 0.07 | 0.38 |
| Mn | 0.36 | *0.60* | 0.90 | 0.07 | 1.00 | 0.43 |
| Ti | 0.31 | *0.58* | 0.54 | 0.38 | 0.43 | 1.00 |

## Spatial mapping of Cr in SX cores

- Moderate to weak correlations exist between total Cr and Fe, Ti and Mn

- Much of the Cr appears to be evenly distributed throughout the samples

# XANES Analysis of Cr(VI):Cr(III) Ratio in Core Samples

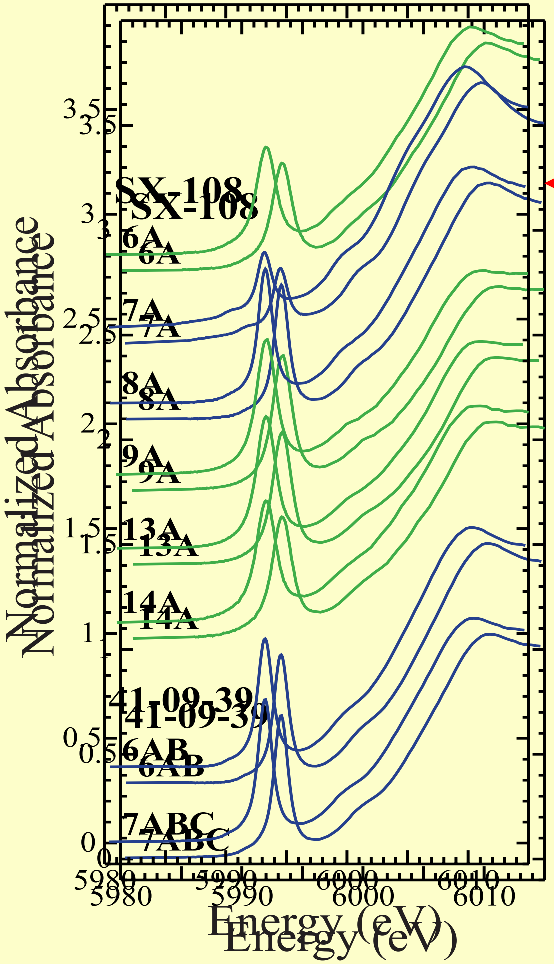


% Cr(VI)

54
25
53
71
69
62

51
58

# Comparison of the extent of Cr reduction to sediment properties

| Sample | % Cr(VI) | Total Cr (ppm)[1] | Cr(VI) (ppm) | pH[2] | Depth b.g.s. (ft) | Total Na (ppm) |
|---|---|---|---|---|---|---|
| ***SX-108 Core*** | | | | | | |
| ***6A*** | 54 | 955 | 516 | 8.0 | 80 | 5631 |
| ***7A*** | **25** | 1297 | 324 | **9.6** | 84 | **21325** |
| ***8A*** | 53 | 2098 | 1112 | 7.8 | 88 | 18383 |
| ***9A*** | 71 | 1394 | 990 | 7.9 | 92 | 8694 |
| ***13A*** | 69 | 931 | 642 | 8.0 | 113 | 8277 |
| ***14A*** | 62 | 388 | 241 | 7.6 | 121 | 8353 |
| ***41-09-39 Core*** | | | | | | |
| ***6AB*** | 51 | 1186 | 605 | 8.3 | 90 | |
| ***7ABC*** | 58 | 2090 | 1212 | 8.7 | 83 | |

[1]as determined by XRF [2]from hot water extract

- Highly reduced sample (7A) has highest pH and highest [Na]; also showed significant alteration
- Most samples similar in pH, [Na]

# Conclusions

1. Sr can be incorporated into/on Al-precipitates.

2. If U(VI) and $Na^+$ are present at sufficient concentrations Na-uranates may be important.

3. Reaction of SX tank fluids near-field may have led to dissolution of silicates with release of Fe(II) and possible formation of zeolites.

# Conclusions

4. Dissolution-induced release of Fe(II) can lead to reduction of Cr(VI) to Cr(III).

5. Cr XANES on field samples indicate some in situ reduction did occur; however it is limited to zone most impacted by high pH. Surface passivation, carbonate coatings or minimal dissolution may all have contributed to the limited reduction that was observed.

6. Most of the Cr in the ground at SX-108 is still Cr(VI). This has important implications for future cleanup.